Advanced Fuel Cycle Initiative	**DOCUMENT RELEASE AUTHORIZATION**	

Argonne National Laboratory
9700 South Cass Avenue
Argonne, IL 60439

ANL AFCI Document Number:	ANL-AFCI-205	Release Date:	September 28, 2007
Title:	Uncertainty in Unprotected Loss-of-Heat-Sink, Loss-of-Flow, and Transient-Overpower Accidents		
Author(s):	Edgar E. Morris		

Approval for Release

Approved by:			**Date**
Principal Author:	Edgar E. Morris	Edgar E. Morris	9-21-07
ANL Work Package Manager:	Robert N. Hill	Robert N. Hill	9-21-07
ANL Program Manager:	Robert N. Hill	Robert N. Hill	9-21-07

Uncertainty in Unprotected Loss-of-Heat-Sink, Loss-of-Flow, and Transient-Overpower Accidents

By

E. E. Morris

Nuclear Engineering Division
Argonne National Laboratory
9700 S. Cass Avenue
Argonne, Illinois 60439

September 28, 2007

Uncertainty in Unprotected Loss-of-Heat-Sink, Loss-of-Flow, and Transient-Overpower Accidents

By

E. E. Morris

Introduction

The sensitivities of various output parameters to selected input parameters in unprotected combined loss of heat-sink and loss-of-flow (ULOHS), loss-of-flow (ULOF), and transient-overpower (UTOP) accidents are explored in this report. This line of investigation was suggested by R. A. Wigeland[1]. For an initial examination of potential sensitivities, the MATWS computer program[2] has been compiled as part of a dynamic link library (DLL) so that uncertain input parameters can be sampled from their probability distributions using the GoldSim simulation software[3]. The MATWS program combines the point-kinetics module from the SAS4A/SASSYS computer code[4] with a simplified representation of the reactor heat removal system. Coupling with the GoldSim software by means of a DLL not only provides a convenient mechanism for sampling the stochastic input parameters but also allows the use of various tools that are available in GoldSim for analyzing the dependence of various MATWS outputs on these parameters. Should a decision be made to continue this investigation, the techniques used to couple MATWS and GoldSim could also be applied to couple the SAS4A/SASSYS computer code[4] with GoldSim. The work described here illustrates the type of results that can be obtained from the stochastic analysis.

Modeling

A MATWS model of an advanced burner reactor with a conversion ratio of approximately 0.5 is used in the calculations. The reactor power is 840 MWth. Balance of plant modeling is the same as developed by Hill and Wigeland for the PRISM Mod B sodium cooled fast reactor[5]. It includes decay heat removal that depends on the reactor vessel temperature but that can remove up to 3.5% of nominal power. The reactor design is similar to the advanced burner reactor having a conversion ration of 0.25, considered by Cahalan, Smith, Hill, and Dunn[6]. Reactivity coefficients used in the model were evaluated by Smith[7]. For the ULOHS and ULOF analysis, reactivity coefficients for an end of equilibrium cycle (EOEC) core were used. The reactivity coefficients used in ULOHS and ULOF analysis are listed in Table 1. Values for the coefficients are assumed to be mean values for a normal distribution. Uncertainties in the coefficients are represented by the standard deviations listed in the table. These standard deviations were assigned arbitrarily, but the values listed are thought to be representative of the magnitude of the uncertainty that would be obtained from a systematic analysis. In addition to the reactivity coefficients, the ULOHS calculations postulated that at when the coolant inlet temperature reached a value of 800 K, coolant pumps in both the primary and intermediate coolant loops would coast down. The trip temperature was assumed to be normally distributed with a mean value of 800 K and a standard deviation of 15 K. Also, the rate

at which heat removal decreases to zero was assigned a normal probability distribution with a mean value of 0.05 s^{-1} and a standard deviation of 0.005 s^{-1}. Values for the trip temperature and the rate of heat removal decrease are also listed in Table 1.

Reactivity coefficients for the UTOP analysis were evaluated for a beginning of equilibrium cycle (BOEC) core. The mean values for the stochastic input parameters are listed in Table 2. Standard deviations for the various reactivity coefficients were left at the same values assigned to the corresponding coefficients for the EOEC core. In the UTOP analysis, a control rod is assumed to be withdrawn introducing reactivity at a constant rate. The reactivity worth and the time required to fully withdraw the rod were assigned normal probability distributions with the mean values and standard deviations listed in Table 2.

The procedure to follow in preparing a Fortran DLL for coupling with GoldSim is described in Appendix C of Ref. 3. As an initial step, the main program of the MATWS code was changed to a FORTRAN subroutine. As a second step, an interface subroutine was developed which receives input parameters from GoldSim, adds these parameters to a standard input file for the MATWS program and rewrites the input file. The interface subroutine then calls the MATWS program and MATWS calculates the desired transient. Following completion of the transient calculation the interface subroutine calls a subroutine which reads a plot file produced by MATWS and extracts the results to be sent back to GoldSim. The simulation times at which results are reported to GoldSim are determined by GoldSim. Calls to the MATWS program and the subroutine for reading the plot file occur on the first GoldSim time step. On subsequent calls to the interface subroutine, the routine interpolates from the MATWS results and reports the interpolated results back to GoldSim. Each independent repetition of the process, sampling the input parameters by GoldSim, the transient calculation by MATWS, and the transfer of all output results back to GoldSim is referred to as a realization. All the calculations considered in this report are based on 10,000 realizations and follow only the first 3590 seconds of the transient.

ULOHS

This accident sequence is initiated by a loss of the ability to remove heat from the intermediate coolant loop. Heat removal in the MATWS model used here is specified by a table giving the heat removal rate as a function of time. The loss of heat removal is modeled by reducing the heat removal linearly to zero at a specified rate. Throughout the period while the heat removal rate is decreasing, the primary and intermediate coolant pumps continue to maintain the nominal flow. As the heat removal rate decreases, the coolant inlet temperature increases. In the model assumed here, when the inlet temperature reaches a value near 800 K, the pumps trip but the scram system fails. The pump trip initiates flow coastdowns in both the primary and intermediate coolant loops. Flow coastdowns are modeled by specifying the coolant flows in the primary and intermediate loops by means of tabular input. The flow halving time is about 4 seconds for the primary coolant loop and approximately 7 seconds for the intermediate loop. Because the MATWS program does not have the ability to dynamically modify the flow coastdown tables, the MATWS calculation is run twice for each realization. In the first calculation no flow coastdown occurs but the time when the coolant inlet temperature reaches the trip temperature is determined. The interface routine then adjusts the flow vs. time tables, writes a new input file for MATWS and runs the second calculation. In the second calculation the flow

coastdowns are initiated at the time when the coolant inlet temperature reaches the trip temperature.

Figure 1 shows the mean normalized power, upper and lower bounds, and various percentiles for the normalized power. At each time, the upper and lower bounds indicate the larges and smallest values of the normalized power among all the realizations evaluated, not the largest and smallest values that could ever occur. Similarly, the curve for a given percentile is, at a given time, the upper bound for the power levels determined on that percentage of the realizations. A percentile curve will seldom correspond to a specific realization for the entire time span. This is illustrated in Fig. 2 which shows the normalized power curves for the first 10 realizations. For the first 300 seconds, realization 4 is the lowest of the 10 curves. From about 500 seconds until nearly 600 seconds it is the second or third highest curve and from about 750 seconds until the end of the transient it is again the lowest curve. Figure 1 shows that with the standard deviations given in Table 1, there is a large spread (factors of six to twelve) between the upper and lower bounds of the power over much of the time period covered in the plot. Plots of mean values and percentiles for the fuel, the coolant inlet, and coolant outlet temperatures are shown in Figs. 3, 4, and 5. For the distributions selected, the earliest pump trip time is approximately 180 s after the heat sink begins to fail. Prior to this time, the coolant inlet temperature is relatively insensitive to all parameters. At 180 s, the upper and lower bounds on the coolant inlet temperature differ by less than 6 K. However, by this time the upper and lower bounds on the outlet coolant temperature differ by about 30 K and on fuel temperature differ by about 64 K. The largest difference between the upper and lower fuel temperature bounds, 179 K, occurs 550 s after the heat removal system begins to fail.

Figure 6 shows the frequency distribution for the peak fuel temperature. It is estimated that the fuel melting temperature is above 1300 K, nearly 300 K larger than the largest fuel temperature found among the 10,000 samples. The frequency distribution for the peak fuel temperature appears to be nearly log-normal in shape. The smooth curve shown in Fig. 6 is a log-normal probability density with the mean and standard deviation as computed from the logarithms of the peak fuel temperatures[*]. Comparison of the histogram with the smooth curve suggests that the log-normal distribution may be a reasonable approximation to the probability distribution for the peak fuel temperature, however, it should be noted that over most of the temperature range included in Fig. 6, the smooth curve lies outside an estimated 99% confidence interval for the frequency distribution. This confidence interval is indicated in the figure by the short horizontal lines above and below each step on the histogram. The interval is estimated by observing that for the temperature interval indicated by each step in the histogram, the number of realizations that fall within that interval is binomially distributed. The probability of falling within a given interval can be approximated by the ratio of the number of realizations in the interval divided by the total number of realizations. Then the probability distribution for the number of realizations in an interval can be represented by a binomial distribution with an expected number of realizations equal to the number actually calculated within the interval and a number of trials equal to the total number of realizations in the calculation. This distribution then can be used to calculate the confidence interval shown in Fig. 6 for the interval. It can be seen that the log-normal distribution falls within the confidence interval only for a small range of

[*] Note that the curves in Fig. 6 integrate to unity when integrated with respect to the logarithm of the temperature.

temperatures around 877 K, a second small range around 905 K, and a third small interval around 933 K.

The frequency distribution for the peak coolant outlet temperature is shown in Fig. 7. Again, the distribution resembles a log-normal distribution and the log-normal distribution having the same mean and standard deviation as the results that give rise to the frequency distribution is shown in the figure. The 99% confidence interval for the frequency distribution is indicated by the short horizontal lines above and below each step in the histogram. As was the case for the peak fuel temperature, over most of the temperature range, the log-normal distribution lies outside the 99% confidence interval. Thus while the log-normal distribution may be a useful approximation to the frequency distribution, the results in Fig. 7 as also in Fig. 6 indicate that the frequency distribution does not arise out of an underlying log-normal distribution.

Scatter plots of the peak coolant outlet temperature against each of the uncertain input parameters are shown in Figs. 8 through 14. These plots indicate relatively weak dependence of the peak outlet temperature on all parameters except the radial core expansion coefficient. Linear regressions for the peak outlet temperature against each of the seven input parameters has a positive slope except for regressions on the control rod driveline expansion reactivity coefficient and on the pump trip temperature. In the case of the control rod driveline expansion coefficient, if the regression had been made on the magnitude of this coefficient, the slope of the regression line would have been positive. At the same time, if the regressions of the peak coolant outlet temperature on the Doppler and fuel axial expansion coefficients had been made against the magnitude of these parameters, the slopes of the regression lines would have been negative. The scatter plot for the peak coolant outlet temperature as a function of the radial core expansion reactivity feedback coefficient (Fig. 13) indicates a non-linear dependence on this parameter.

Table 3 lists GoldSim-calculated values for various measures of the importance of individual input parameters to the peak coolant outlet temperature. The results in the table quantify the observations in the foregoing paragraph. Correlation coefficients were determined by linear regression of the peak coolant outlet temperature on each of the seven input parameters listed in the table. The standardized regression coefficients are based on a linear regression of the standardized peak coolant outlet temperature on the standardized value of each input parameter. A standardized parameter is the ratio of the difference between the parameter and its mean value to the standard deviation of the parameter. Partial correlation coefficients between the peak coolant outlet temperature and one of the input parameters are determined by first computing the separate regressions of the peak coolant outlet temperature and of the input parameter on the remaining input parameters. The partial correlation coefficient is then the correlation coefficient for the residuals of these two regressions. Finally, values for the importance measure for a given input parameter are determined by computing the variance of the peak fuel temperature for given values of the input parameter and then computing the average value of the variances so determined. The correlation coefficients, standardized regression coefficients, and the partial correlation coefficients all agree that the ranking of the stochastic input parameters in descending order of importance is 1) radial core expansion, 2) coolant reactivity coefficient, 3) fuel axial expansion reactivity coefficient, 4) Doppler reactivity coefficient, 5) rate of heat removal decrease, 6) inlet coolant trip temperature, and 7) control rod

expansion reactivity coefficient. In the case of the importance measure in the last column of the table, the ranking is modified to 4) control rod expansion reactivity coefficient, 5) inlet coolant trip temperature, 6) Doppler reactivity coefficient, and 7) rate of heat removal decrease. Each of the importance indicators listed in Table 3 show the same relative importance of the

A table similar to Table 3, but for the peak fuel temperature instead of the peak coolant outlet temperature, shows the same relative importance for the reactivity coefficients and ranks radial core expansion, coolant reactivity coefficient, fuel axial expansion, and inlet coolant trip temperature, respectively, as the first, second, third, and fourth most important parameters. However, the correlation coefficients, standardized regression coefficients, and partial correlation coefficients rank the remaining input parameters in descending order of importance as Doppler reactivity coefficient, rate of heat removal decrease, and control rod expansion reactivity coefficient while the importance measure of the fourth column moves the control rod expansion reactivity coefficient ahead of the Doppler reactivity coefficient and the rate of heat removal decrease.

ULOF

The ULOF is initiated when pumps in both the primary and intermediate coolant loops begin a coastdown. It is postulated that the scram system fails so that the only mechanism for bringing the reactor power down from its nominal level is the reactivity feedbacks built into the reactor system. The coolant flow during the coastdown is determined by tabular input to the MATWS computer code. As in the latter part of the ULOHS, the flow halving times are approximately 4 and 7 seconds, respectively, for the primary and intermediate coolant loops. It is further postulated that the loss of flow in the primary and intermediate coolant loops is accompanied by a reduction in the flow of water in the steam generator so that heat removal from the intermediate loop is degraded. This reduction in heat removal is simulated by linearly reducing the rate of heat removal from the intermediate loop to zero over a period of about 20 seconds. The heat reduction rate is also specified by means of tabular input to the MATWS code.

Upper and lower bounds as well as the mean and selected percentile curves for the normalized power in a ULOF are shown in Fig. 15. The largest difference between upper and lower bounds on the power is much smaller than in the case of the ULOHS, ranging up to only about a factor of 2.5. Figures 16, 17, and 18 show mean and percentile plots of the fuel, coolant inlet, and the coolant outlet temperatures. The maximum difference, 130 K, between the largest and smallest fuel temperatures is also smaller than in the case of the ULOHS. Over the first hour or so of the transient, the difference between the upper and lower bounds for the coolant inlet temperature is less than 30 K while for the coolant outlet temperature it is 235 K.

Frequency distributions for the peak fuel temperature and the peak coolant outlet temperature are shown, respectively, in Figs. 19 and 20. Estimated 99% confidence limits are indicated by the horizontal lines above and below each step of the histogram. Also shown are log-normal distributions with the same means and standard deviations as for the results represented by the histograms. As was the case for the ULOHS, the log-normal distribution lies outside the 99% confidence limits over most of the temperature ranges shown in the figures. Nevertheless, the log-normal distribution might be a useful approximation for the distribution of

the peak coolant temperature. Unlike the case for the ULOHS, it would be a very poor approximation for the distribution for the peak fuel temperature.

Table 4 lists several measures of the importance, as calculated by GoldSim, of various input parameters to the peak outlet coolant temperature. Just as in the case of the ULOHS accident, the core radial expansion reactivity coefficient is found to be the most important parameter in determining the peak outlet coolant temperature. The coolant density reactivity feedback is the second most important for the ULOF, also in agreement with the results reported in Table 3 for the ULOHS accident. The various measures are larger for the radial core expansion reactivity coefficient in the ULOF case than in the ULOHS case and smaller for the coolant density reactivity feedback in the ULOF case than in the ULOHS case. It is not known, however, whether these differences are significant. Note, that since heat removal through the steam generator is assumed to cease in both the ULOHS and the ULOF accident sequences, it was retained as a stochastic parameter in the ULOF case. The importance measures shown in Tables 3 and 4 indicate that the behavior of the steam generator may be more important to the ULOF sequence in determining the peak outlet coolant temperature than to the ULOHS sequence. All measures of importance in Table 4 except for the importance measure in the last column indicate that the control rod driveline expansion reactivity feedback is the third most important variable in determining the peak outlet coolant temperature. The importance measure in the last column indicates that the fuel axial expansion reactivity feedback is the third most important parameter. However, the importance measures for radial core expansion and coolant density reactivity feedbacks are considerably larger than the measures for the other parameters.

A table of importance measures for the peak fuel temperature, not shown here, indicates that the two most important determinants of the peak fuel temperature are radial core expansion and coolant density reactivity feedbacks with radial core expansion being the most important. However, unlike the case for the peak coolant outlet temperature, the third most important parameter for the peak fuel temperature is the fuel axial expansion reactivity feedback coefficient. Importance measures for the remaining stochastic input parameters are much smaller than the measures for these three parameters.

UTOP

A UTOP accident sequence initiates when a control rod begins to move out of the reactor core. This event fails to initiate a reactor scram and the coolant pumps continue to maintain the nominal flow through the primary and intermediate coolant loops. Figure 21 shows the normalized reactor power for this transient. As in previous plots of the normalized power, the figure shows the mean, upper and lower bounds, and curves for various percentiles. When the control rod begins to move out of the core, the reactor power increases and continues to increase until after the rod is fully withdrawn. Then the various reactivity feedback mechanisms act to adjust the reactivity back to zero, however, when this is accomplished, the reactor power achieves a steady state at a level higher than nominal. Figures 22, 23, and 24 show similar plots for the fuel, coolant inlet, and coolant outlet temperatures. Both the normalized power and the fuel temperature reach higher levels than in the ULOHS and the ULOF transients, but the coolant temperatures are lower. During the first hour or so, the coolant inlet temperature rises at most only about 20 K and is leveling off when the calculation was stopped.

Frequency distributions for the peak fuel temperature and the peak coolant outlet temperature are shown in Figs. 25 and 26, respectively. The 99% confidence interval is indicated by the horizontal lines above and below each step of the histograms. Log-normal distributions having the same mean and standard deviation as the results used to construct the histograms are shown in the plots. These log-normal distributions lie outside the 99% confidence intervals over most of the temperature ranges shown in the plots.

Scatter plots of the peak fuel temperature as function of the various stochastic input parameters are shown in Figs. 27 – 33. These plots show that the total worth of the control rod and the fuel axial expansion reactivity feedback exert the strongest influence on the peak fuel temperature, with axial expansion exerting the strongest influence. According to the plots, there is a definite positive correlation between the peak fuel temperature and the radial core expansion, but this dependence is not as dramatic as was seen in Fig. 13 for the ULOHS transient. The correlations between the peak fuel temperature and the input variables are quantified in the second column of Table 5. All the remaining measures in Table 5 agree that the three most important determinants of the peak fuel temperature are 1) fuel axial expansion reactivity feedback, 2) the worth of the control rod that is withdrawn, and 3) the radial expansion reactivity feedback. All except the measure listed in the last column of the table agree that the fourth most important is the Doppler reactivity feedback. The Doppler coefficient plays a less important role in the transient considered here because, as indicated in Table 2, it is considerably smaller than the fuel axial expansion feedback coefficient and both these feedbacks are driven by the fuel temperature.

Conclusions

As noted earlier, standard deviations for the normal probability distributions were assigned arbitrarily since systematic evaluations were not available. While the values selected are thought to be representative of the kind of values that would result from a more rigorous evaluation, the main purpose of the values used here is to illustrate the potential utility of a probabilistic analysis of uncertainty in reactor safety calculations. The analysis not only shows the range of possible values of various outputs such as the reactor power and fuel and coolant temperatures, but it also provides a means of estimating the probability of achieving results in various parts of the range as well as of achieving results outside the range. For example, the frequency distributions obtained for the peak fuel temperature and the peak outlet coolant temperature provide a means of estimating probability distributions for the margin to fuel melting or coolant boiling. In addition, it is possible to quantify the relative importance of various uncertain input parameters to accident outcomes.

If in future work it is decided to use a higher fidelity reactor safety code, such as SAS4A/SASSYS, it may not be possible to evaluate the large number of realizations considered in this report. Thus, it would be useful to know what probability distributions various output parameters might have. For example, if one knew a priori that the distributions were normal or log-normal, then in the stochastic analysis it would be sufficient to obtain reasonable estimates of the mean and standard deviation for the output. For the frequency distributions for the peak fuel temperature and the peak coolant outlet temperature, in most cases a log-normal distribution appear to provide a fairly reasonable approximation. However, in no case did the log-normal distribution fall within estimated 99% confidence limits for more than a small portion of the

temperature range, and in one case, that of the peak fuel temperature in a ULOF transient, the log-normal distribution was a very poor approximation the to calculated frequency distribution. Although not described earlier in this report, in the case of the peak coolant outlet temperature in a UTOP transient, a beta distribution was found to provide a better approximation to the calculated frequency distribution. However, the use of this probability distribution requires knowledge not only the mean and standard deviation, but also reliable estimates of the minimum and maximum values of the temperature. The more information required to determine the distribution, the heavier the computational burden will be.

For all the calculations described in this report, the stochastic input parameters were assumed to be independent of one another. In fact, there are likely to be correlations among some of the reactivity coefficients and perhaps among other parameters as well. Some exploration of the potential impact of correlations was made. For example, if there were a strong positive correlation between the radial core expansion and the fuel axial expansion reactivity coefficients, it was found that the frequency distribution for the peak coolant outlet temperature in the ULOHS transient broadened and that the high temperature tail of the distribution extended into the coolant boiling range. Whether or not such a correlation is reasonable and, if so, what the strength of the correlation should be was not determined. Appropriate models for potential correlations should be investigated.

References

1. R. A. Wigeland to J. E. Cahalan, Personal Communication (February 2007).

2. J. E. Cahalan, Personal Communication (June 2002).

3. GoldSim Technology Group, GoldSim Probabilistic Simulation Environment User's Guide, Version 9.50 (October 2006). (Information regarding the GoldSim computer code can be found at www.goldsim.com.)

4. J. E. Cahalan, A. M. Tentner, and E. E. Morris, "Advanced LMR Safety Analysis Capabilities in the SASSYS-1 and SAS4A Computer Codes", Proceedings of the International Topical Meeting on Advanced Reactors Safety, Pittsburgh, PA, April 17-21, American Nuclear Society, 1994.

5. R. N. Hill and R. A. Wigeland, Personal Communication (September 1993).

6. J. E. Cahalan, M. A. Smith, R. N. Hill, and F. E. Dunn, "Physics and Safety Studies of a Low Conversion Ratio Sodium Cooled Fast Reactor," *Physor 2004 – The physics of Fuel Cycles and Advanced Nuclear Systems: Global Developments*, Chicago, Illinois, April 25 – 29, 2004, on CD-ROM, American Nuclear Society, Lagrange Park, Illinois (2004).

7. M. A. Smith, Personal Communication (June 2003).

Table 1
Mean and standard deviations for the normally distributed parameters considered in the uncertainty analysis for ULOHS and ULOF analysis for EOEC.

Parameter	Mean	Standard Deviation
Rate of Heat Removal Decline, s^{-1}	0.05	0.005
Trip Temperature, K	800	15
Coolant Temperature Reactivity Feedback, \$/K	0.00155	0.0002
Doppler Coefficient, $T\,dk/dT$	-0.00207	0.0003
Fuel Axial Expansion Reactivity Feedback, \$/K	-0.00243	0.0006
Radial Core Expansion Reactivity Feedback, \$/K	-0.00292	0.0006
Control Rod Driveline Expansion Reactivity Feedback, \$/m	-45.1	4.5

Table 2
Mean and standard deviations for the normally distributed parameters considered in the uncertainty analysis for UTOP for BOEC.

Parameter	Mean	Standard Deviation
Time for Control Rod Withdrawal, s	22.3	2.23
Control Rod Worth, \$	0.445	0.0445
Coolant Temperature Reactivity Feedback, \$/K	0.00142	0.0002
Doppler Coefficient, $T\,dk/dT$	-0.00192	0.0003
Fuel Axial Expansion Reactivity Feedback, \$/K	-0.00258	0.0006
Radial Core Expansion Reactivity Feedback, \$/K	-0.00310	0.0006
Control Rod Driveline Expansion Reactivity Feedback, \$/m	-53.5	4.5

Table 3
Importance measures for the peak outlet coolant temperature
as reported by GoldSim for a ULOHS event.*

Parameter	CC	SRC	PC	IM
Rate of HR Decline	-0.004	-0.001	-0.005	0.008
Trip Temperature	-0.06	-0.06	-0.268	0.013
Coolant Temperature	0.307	0.304	0.817	0.104
Doppler Coefficient	0.051	0.047	0.215	0.011
Fuel Axial Expansion	0.228	0.238	0.743	0.063
Radial Core Expansion	0.883	0.887	0.972	0.796
Control Rod Driveline	-0.131	-0.128	-0.511	0.026

* CC = correlation coefficient, SRC = standardized regression coefficient, PC = partial correlation coefficient, IM = importance measure.

Table 4
Importance measures for the peak outlet coolant temperature
as reported by GoldSim for a ULOF event.*

Parameter	CC	SRC	PC	IM
Coolant Temperature	0.21	0.21	0.724	0.047
Doppler Coefficient	-0.007	-0.009	-0.045	0.003
Fuel Axial Expansion	-0.072	-0.058	-0.279	0.006
Radial Core Expansion	0.955	0.954	0.979	0.923
Control Rod Driveline	0.036	0.032	0.158	0.001
Rate of HR Decline	0.008	0.013	0.066	0.003

* CC = correlation coefficient, SRC = standardized regression coefficient, PC = partial correlation coefficient, IM = importance measure.

Table 5
Importance measures for the peak fuel temperature
as reported by GoldSim for a UTOP event.*

Parameter	CC	SRC	PC	IM
Coolant Temperature	0.076	0.080	0.357	0.007
Doppler Coefficient	0.132	0.133	0.537	0
Fuel Axial Expansion	0.693	0.710	0.959	0.482
Radial Core Expansion	0.345	0.362	0.865	0.120
Control Rod Driveline	0.004	0.023	0.108	0
Control Rod Worth	0.553	0.572	0.939	0.300
Withdrawal Time	-0.013	-0.007	-0.034	0

* CC = correlation coefficient, SRC = standardized regression coefficient, PC = partial correlation coefficient, IM = importance measure.

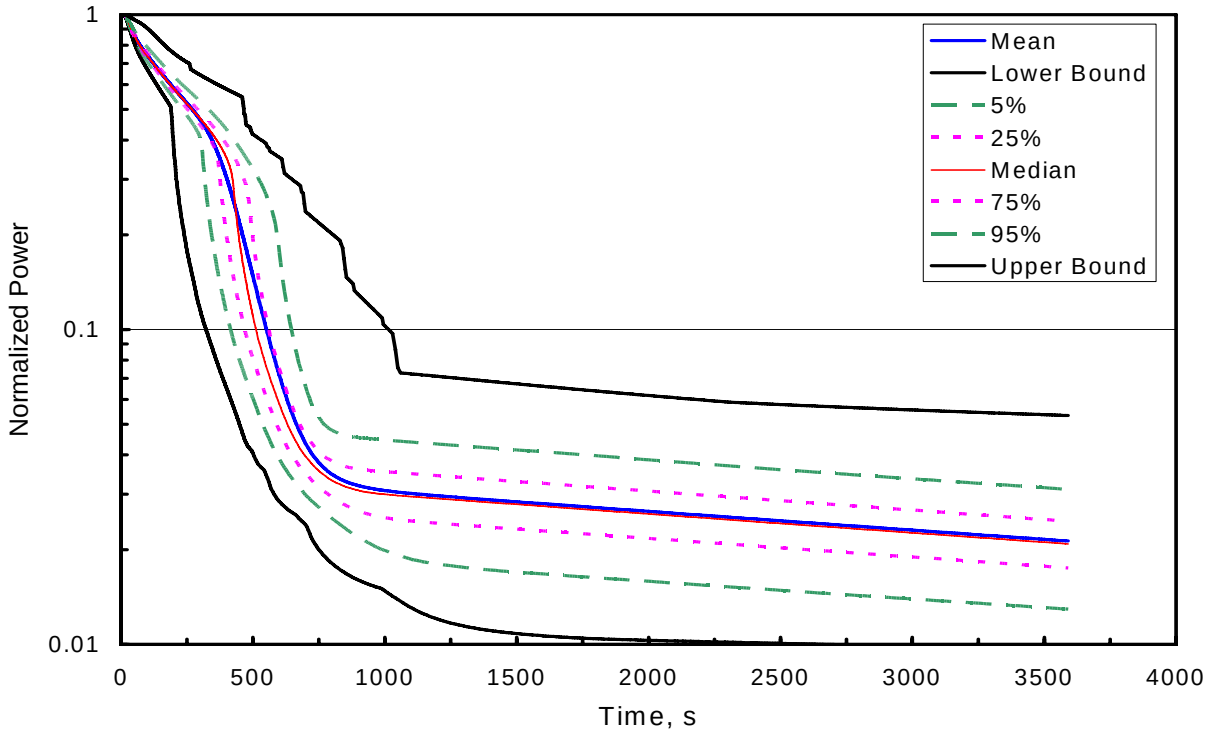

Fig. 1 Mean, percentiles and upper and lower bounds for the normalized power in a ULOHS transient.

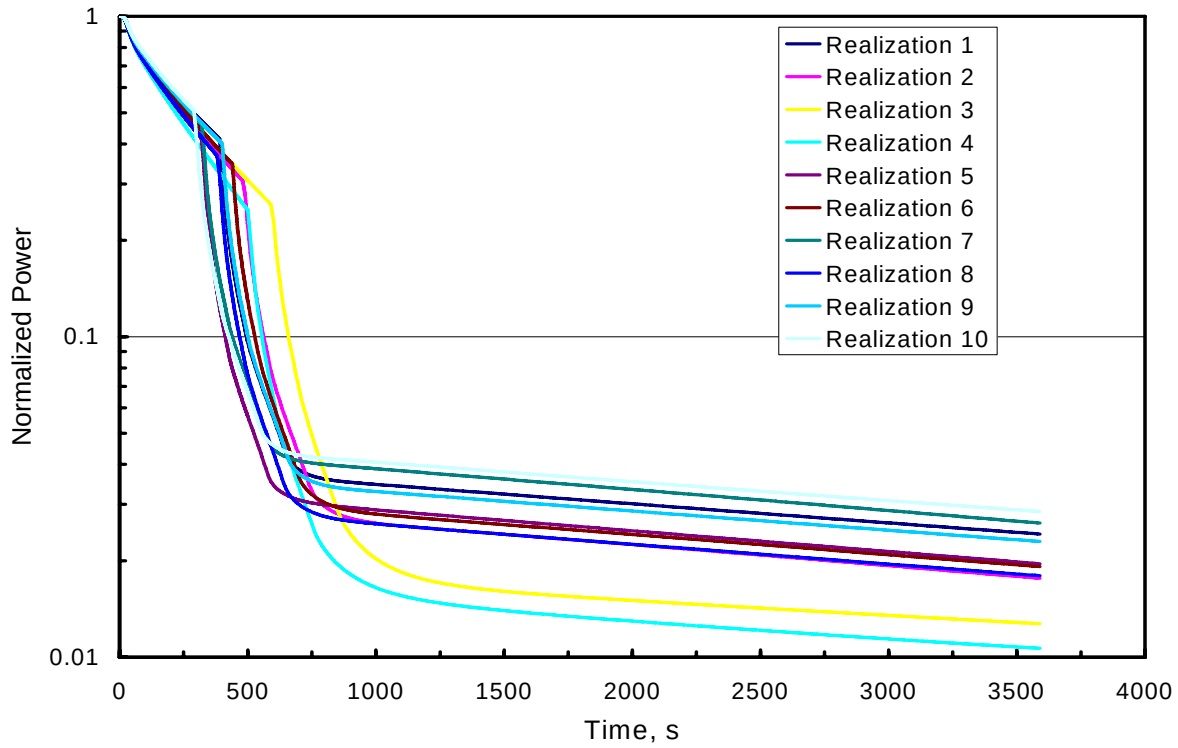

Fig. 2. Normalized power for the first 10 realizations of the ULOHS transient.

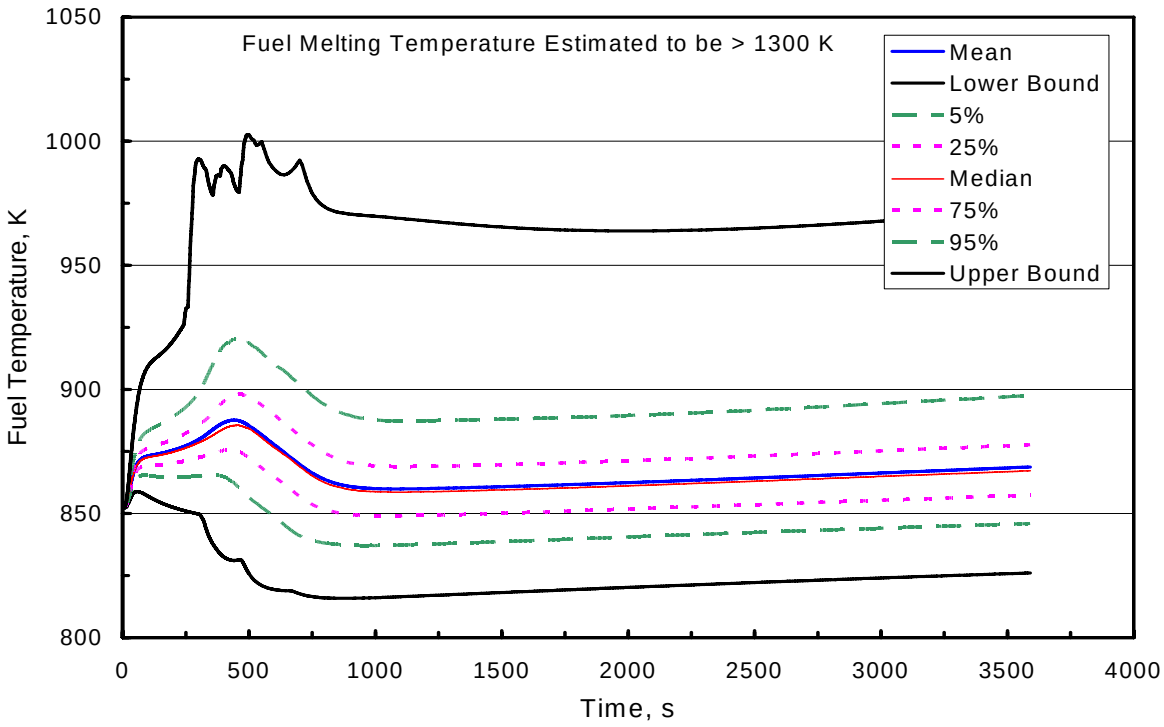

Fig. 3. Mean, percentiles and upper and lower bounds for the fuel temperature in a ULOHS transient.

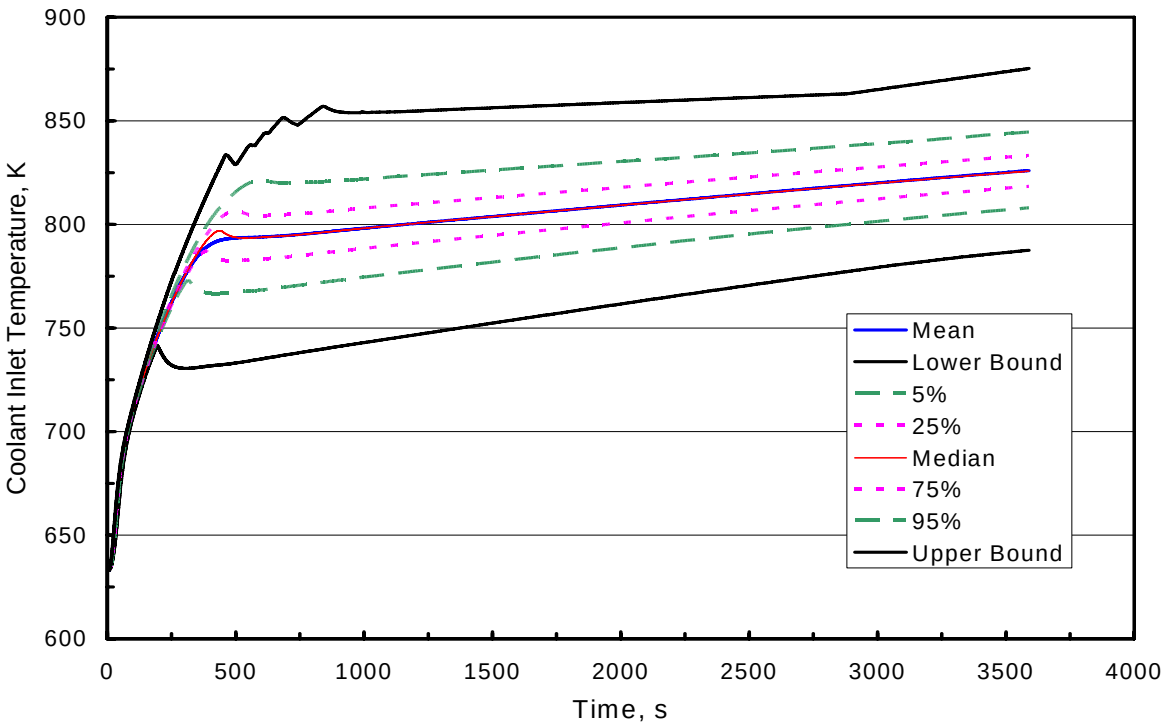

Fig. 4. Mean, percentiles and upper and lower bounds for the coolant inlet temperature in a ULOHS transient.

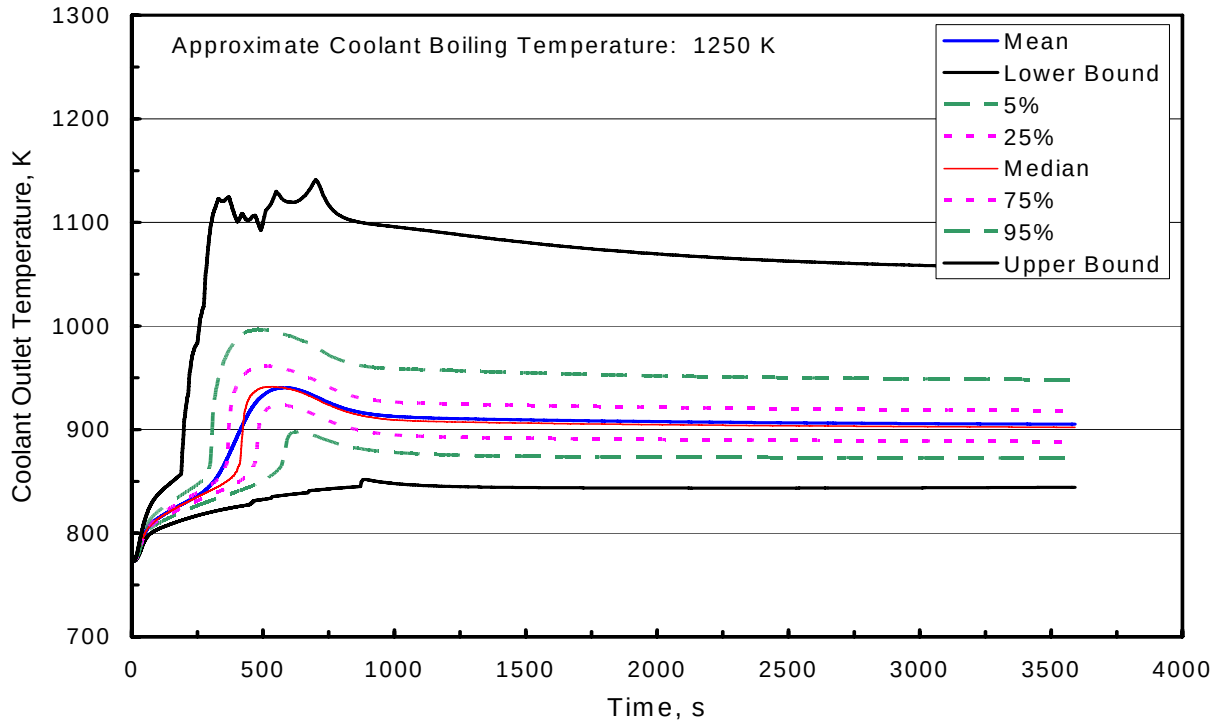

Fig. 5 Mean, percentiles and upper and lower bounds for the coolant outlet temperature in a ULOHS transient.

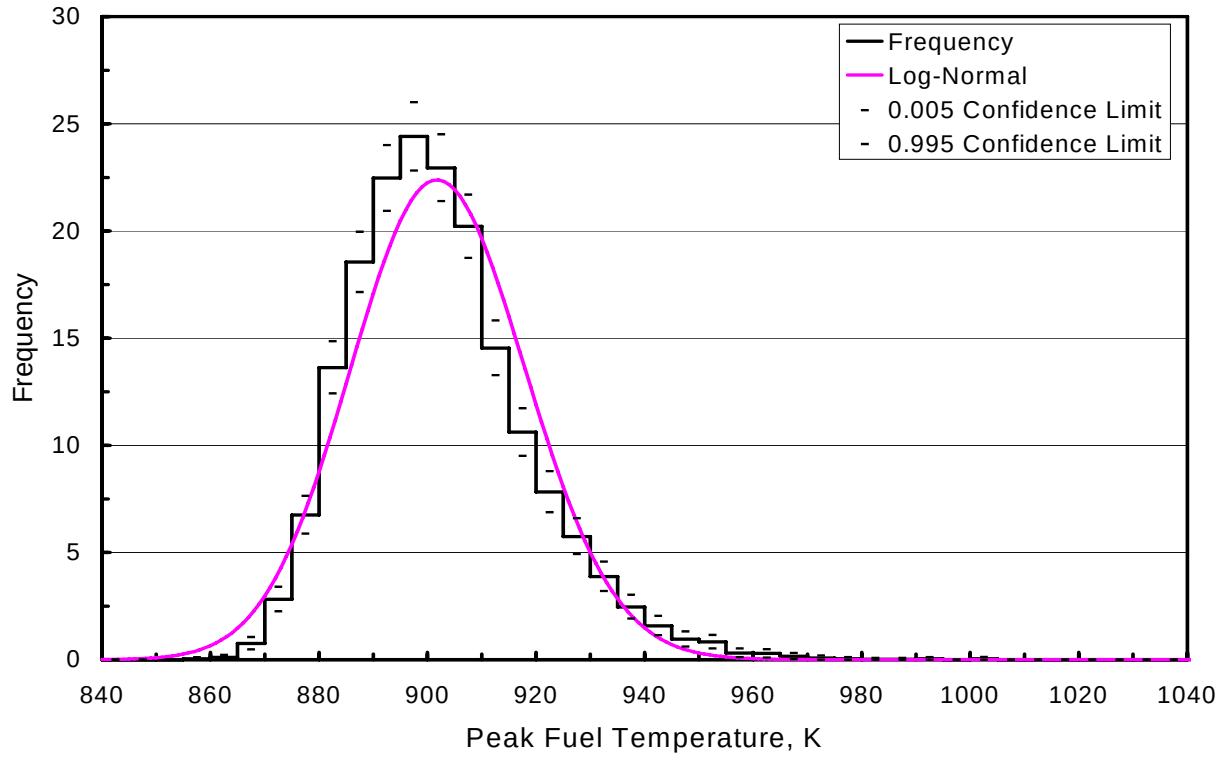

Fig. 6. Frequency distribution for the peak fuel temperature in a ULOHS transient.

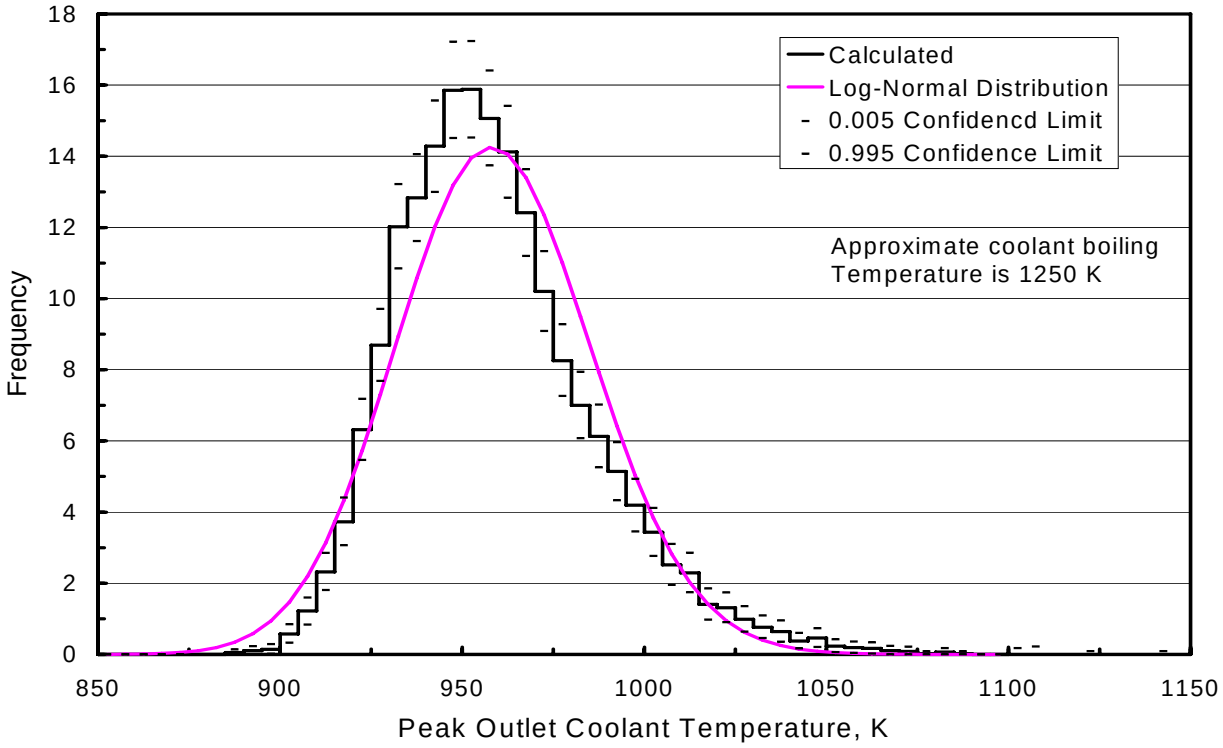

Fig. 7. Frequency distribution for the peak outlet coolant temperature in a ULOHS transient.

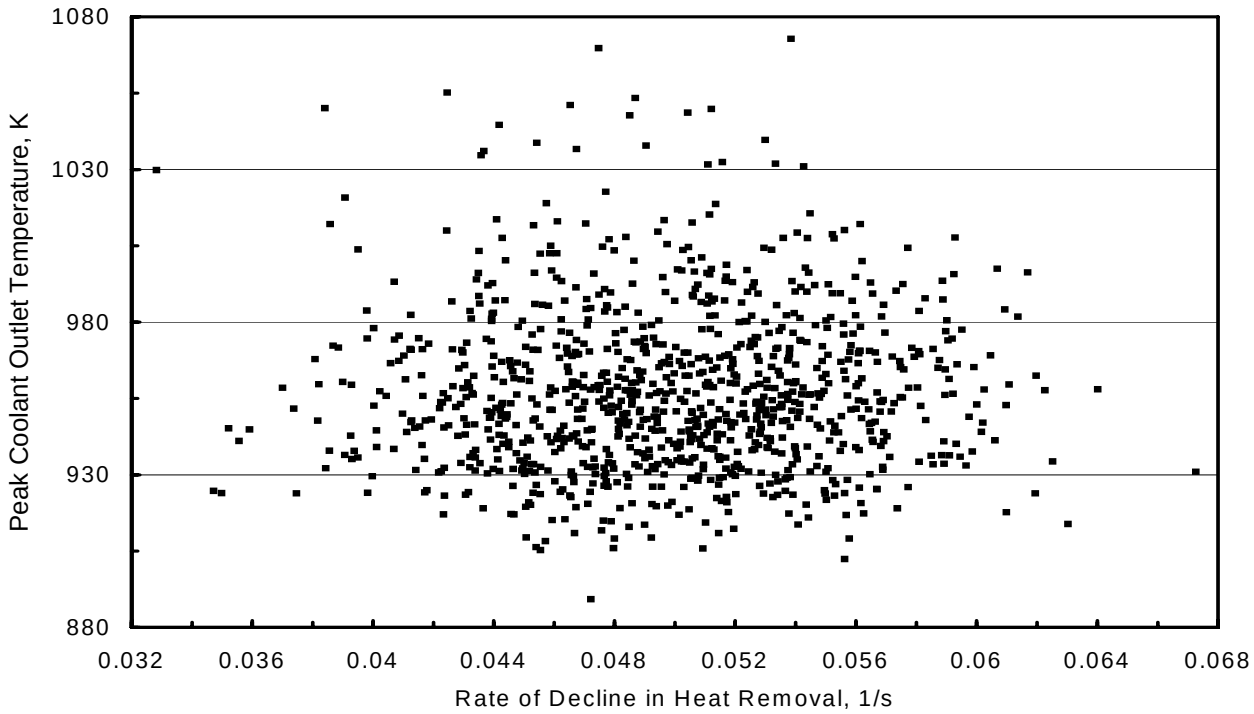

Fig. 8. Peak coolant outlet temperature and the rate of heat removal decline for the first 1000 realizations in a ULOHS transient.

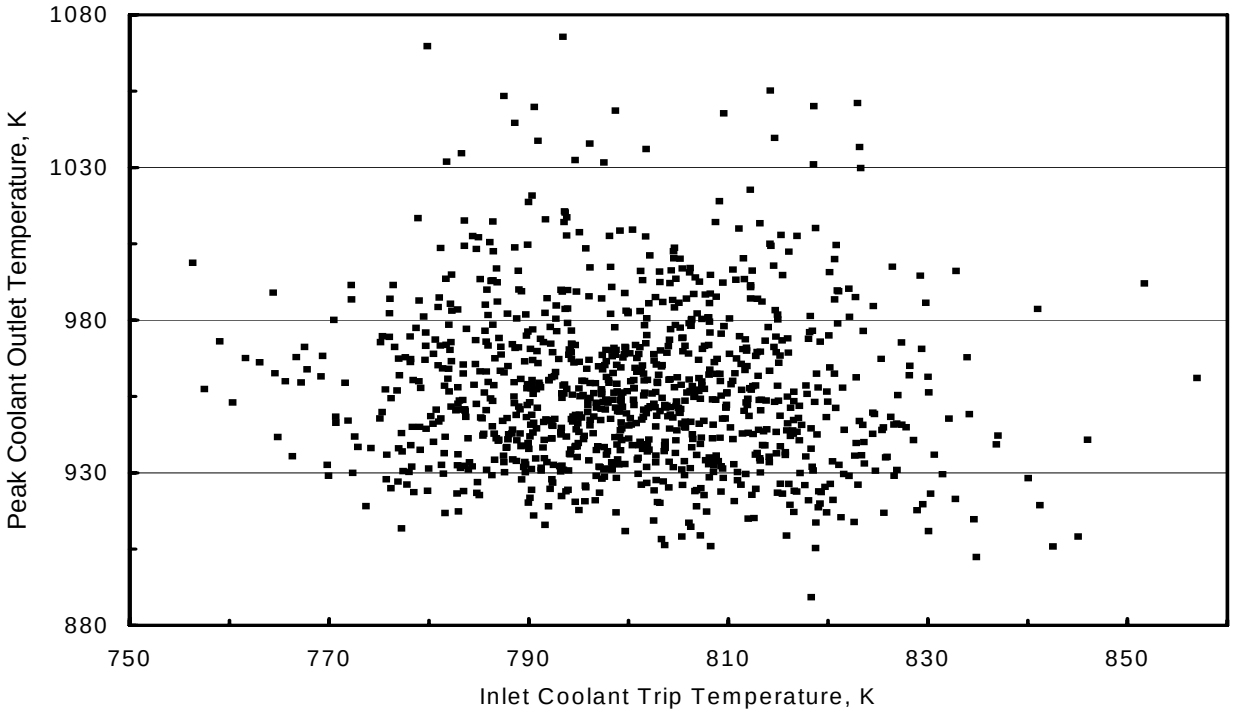

Fig. 9. Peak coolant outlet temperature and the pump trip temperature for the first 1000 realizations in a ULOHS transient.

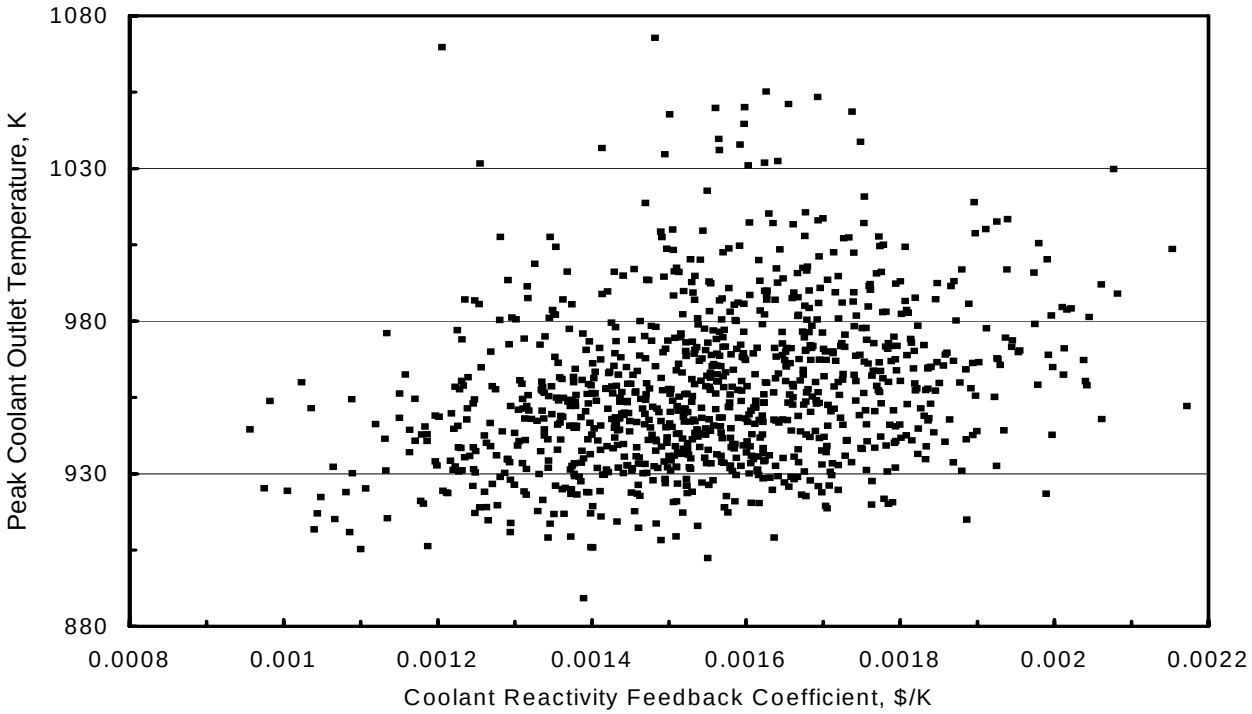

Fig. 10. Peak coolant outlet temerature and the coolant temperature reactivity feedback coefficient for the first 1000 realizations in a ULOHS transient.

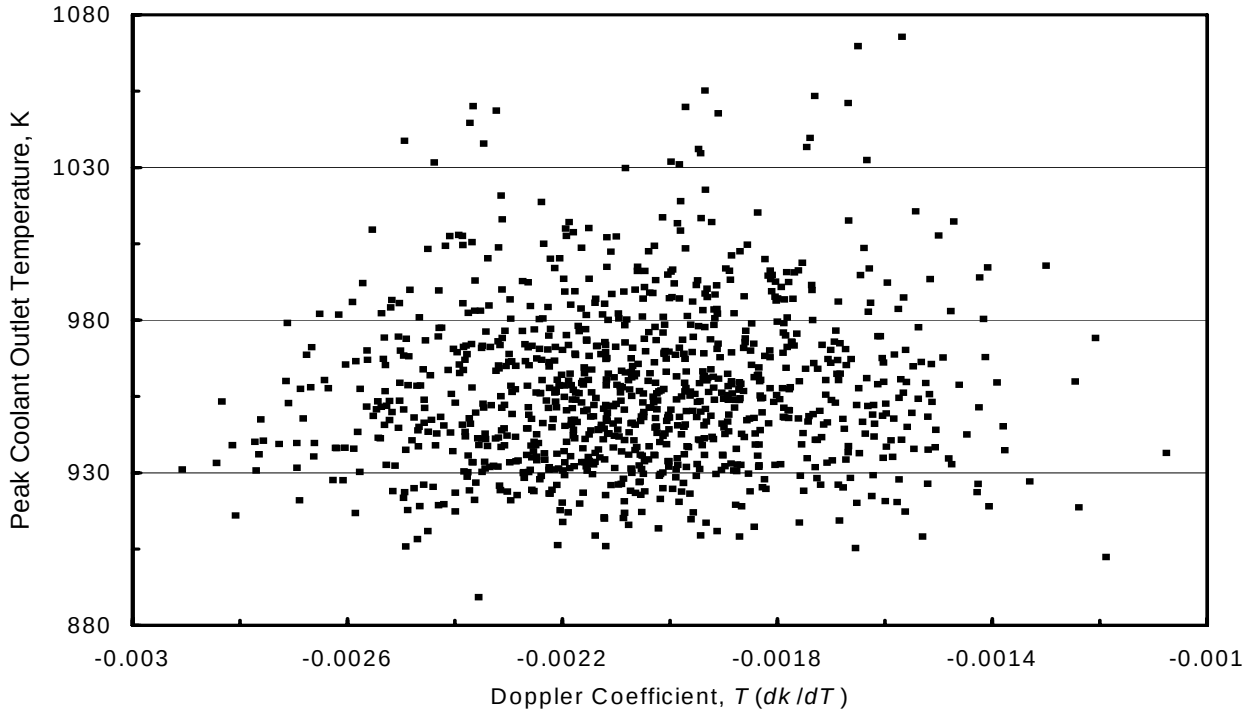

Fig. 11. Peak coolant outlet temperature and the Doppler reactivity feedback coefficient for the first 1000 realizations in a ULOHS transient.

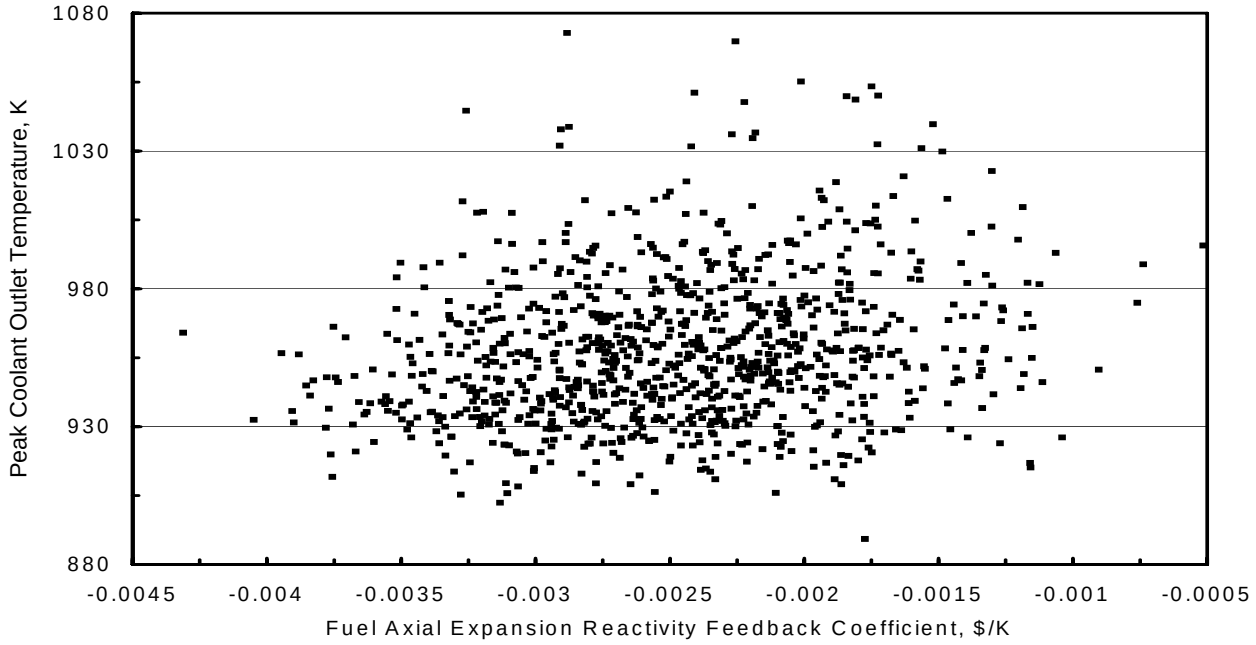

Fig. 12. Peak coolant outlet temperature and the fuel axial expansion reactivity feedback coefficient for the first 1000 realizations in a ULOHS transient.

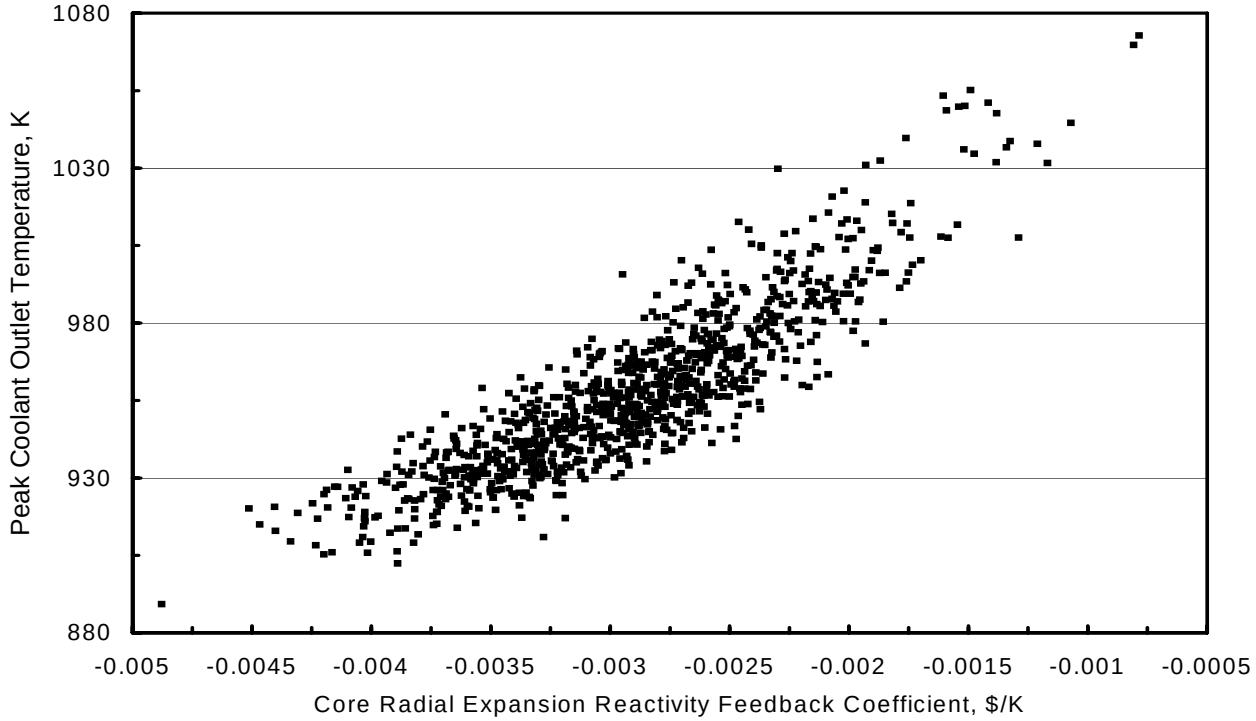

Fig. 13. Peak coolant outlet temperature and the core radial expansion reactivity feedback coefficient for the first 1000 realizations in a ULOHS transient.

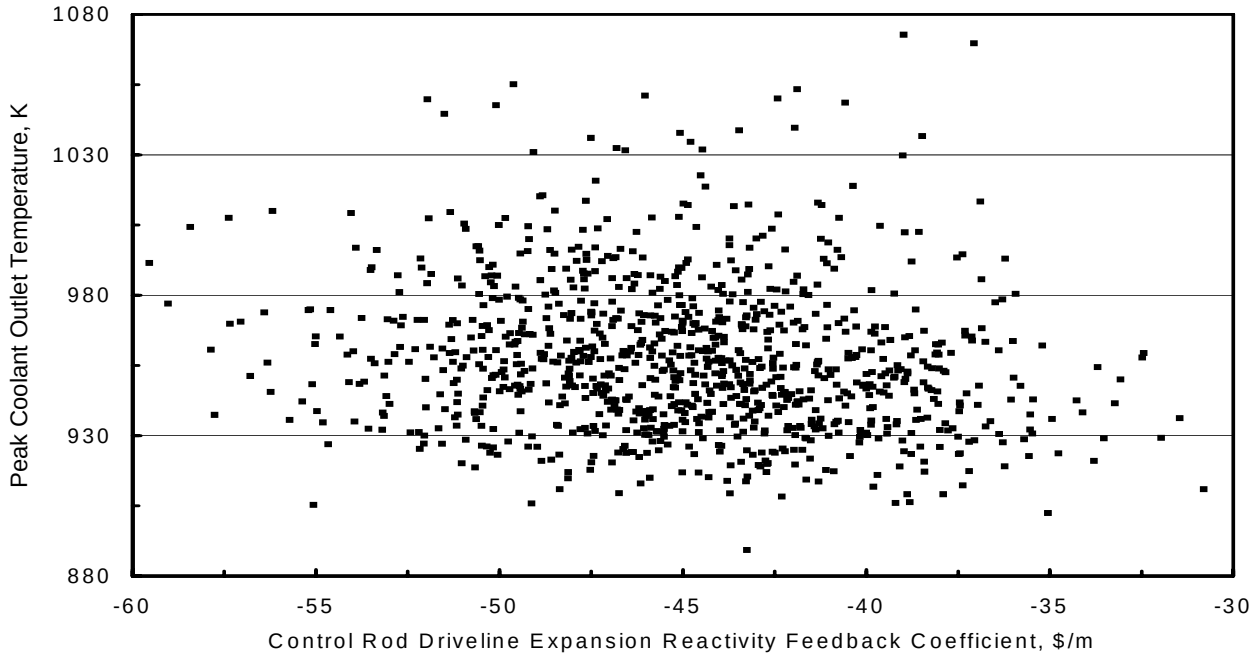

Fig. 14. Peak coolant outlet temperature and the control rod driveline expansion reactivity feedback coefficient for the first 1000 realizations in a ULOHS transient.

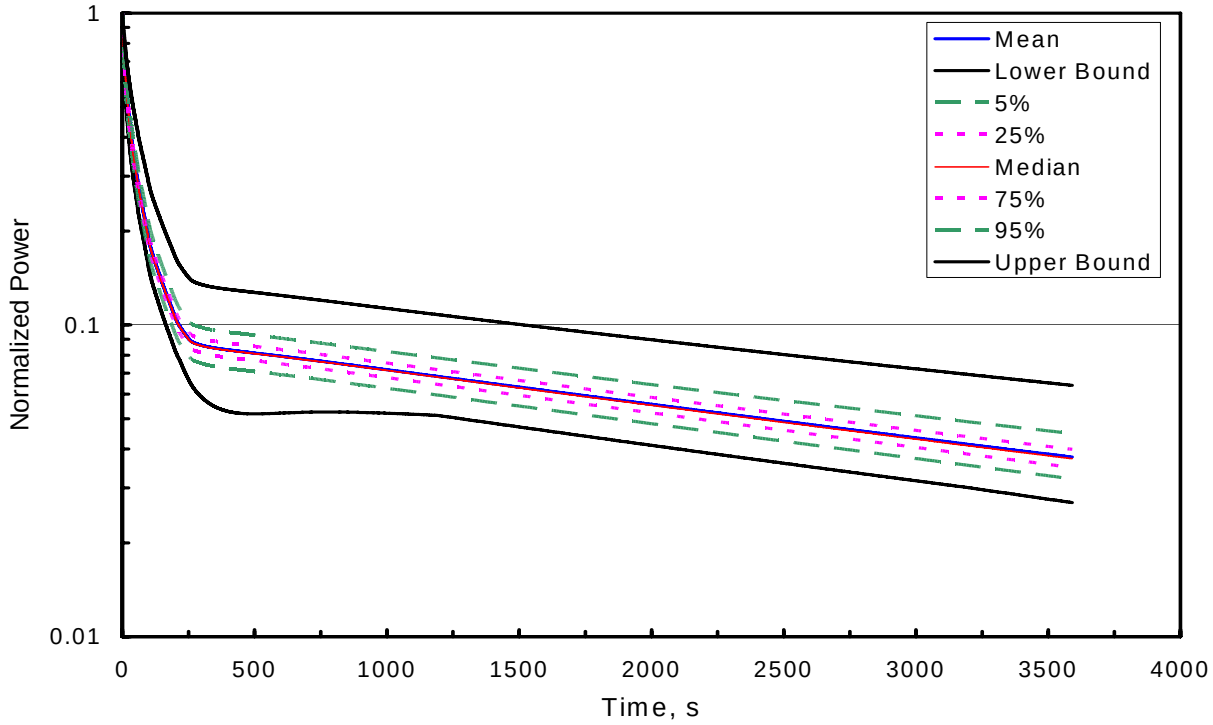

Fig. 15. Mean, percentiles and upper and lower bounds for the normalized power in a ULOF transient.

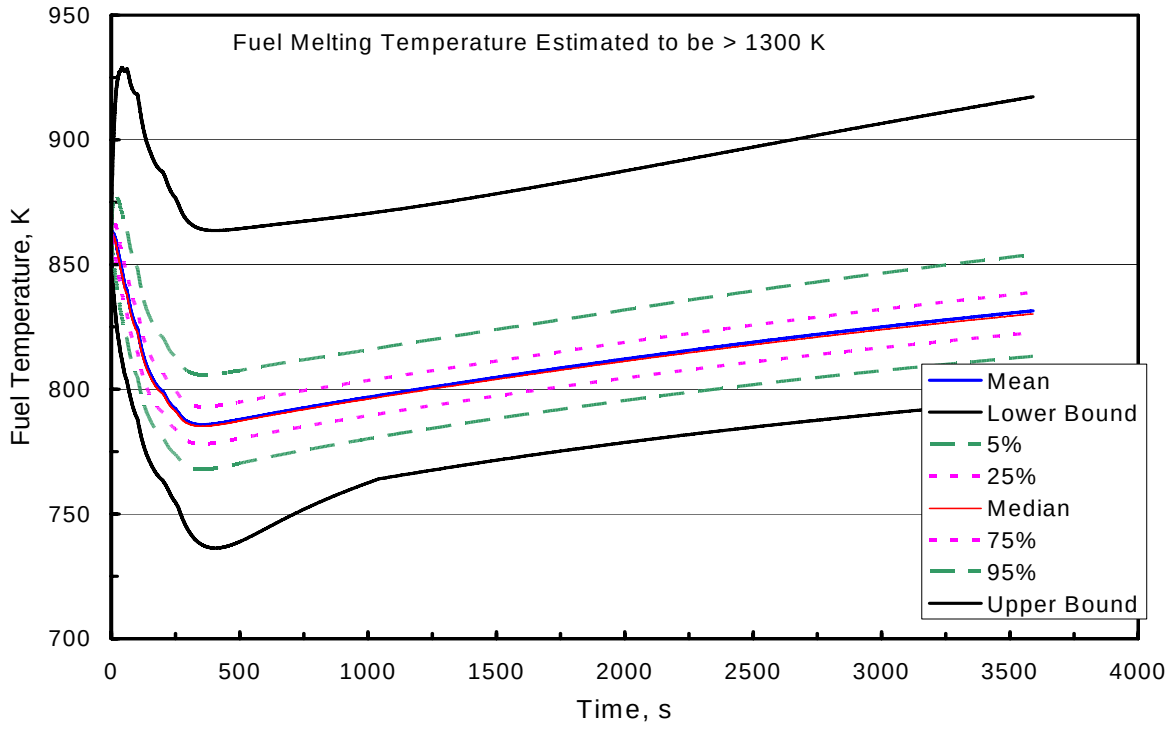

Fig. 16. Mean, percentiles and upper and lower bounds for the fuel temperature in a ULOF transient.

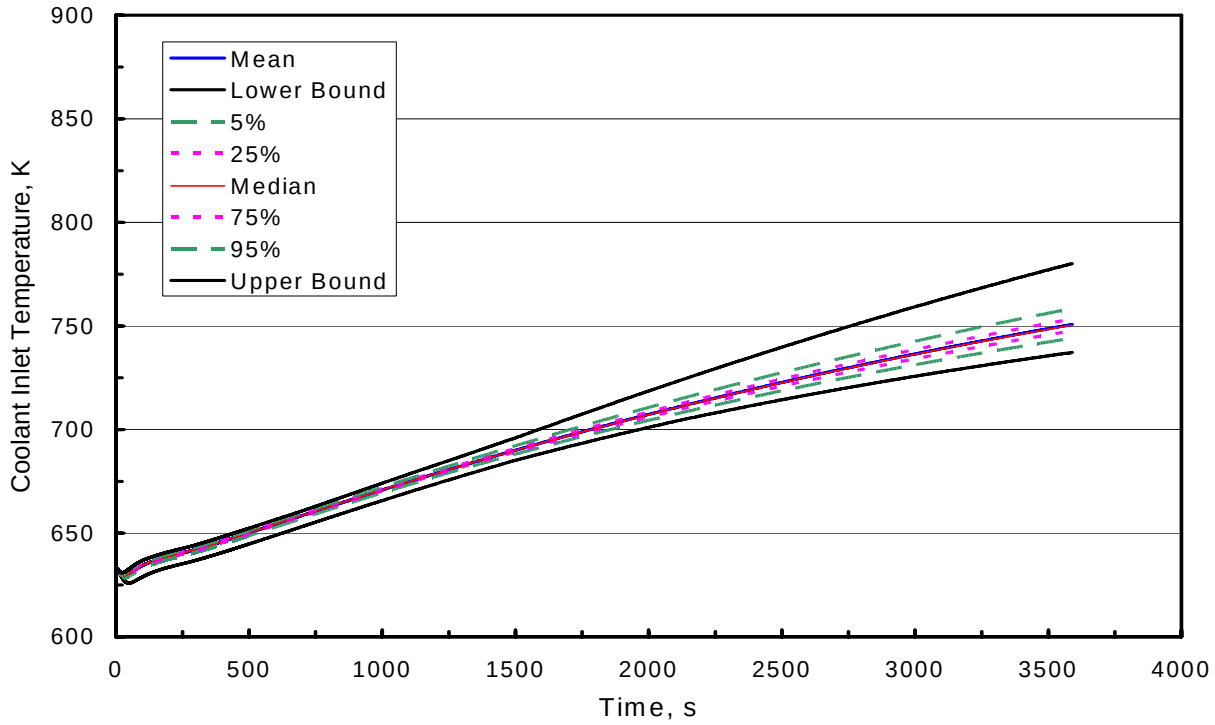

Fig. 17. Mean, percentiles and upper and lower bounds for the coolant inlet temperature in a ULOF transient.

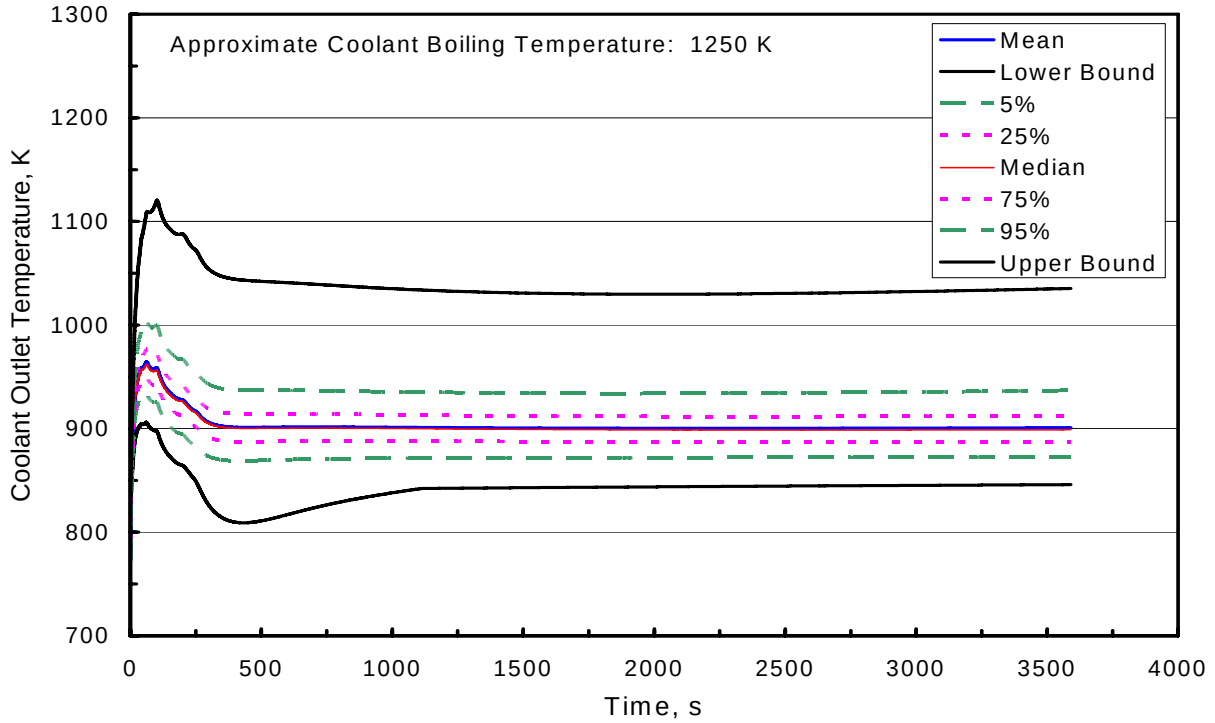

Fig. 18. Mean, percentiles and upper and lower bounds for the coolant outlet temperature in a ULOF transient.

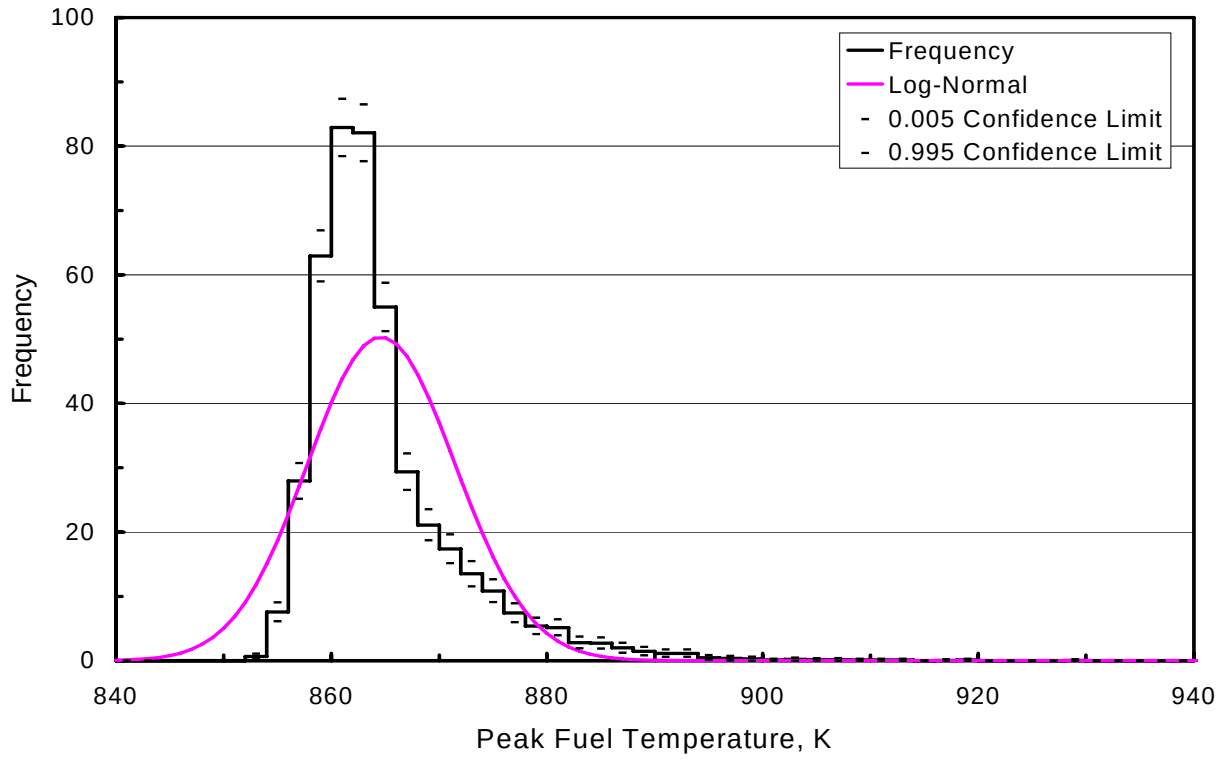

Fig. 19. Frequency distribution for the peak fuel temperature in a ULOF transient.

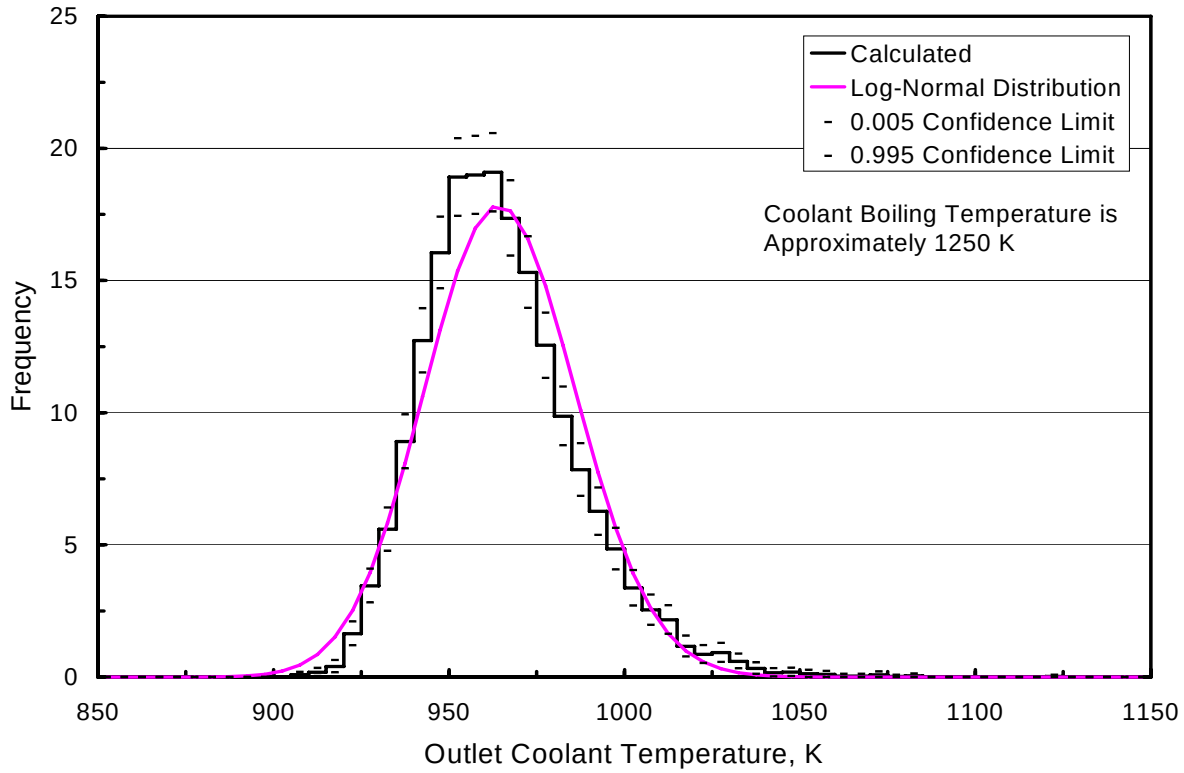

Fig. 20. Frequency distribution for the peak outlet coolant temperature in a ULOF transient.

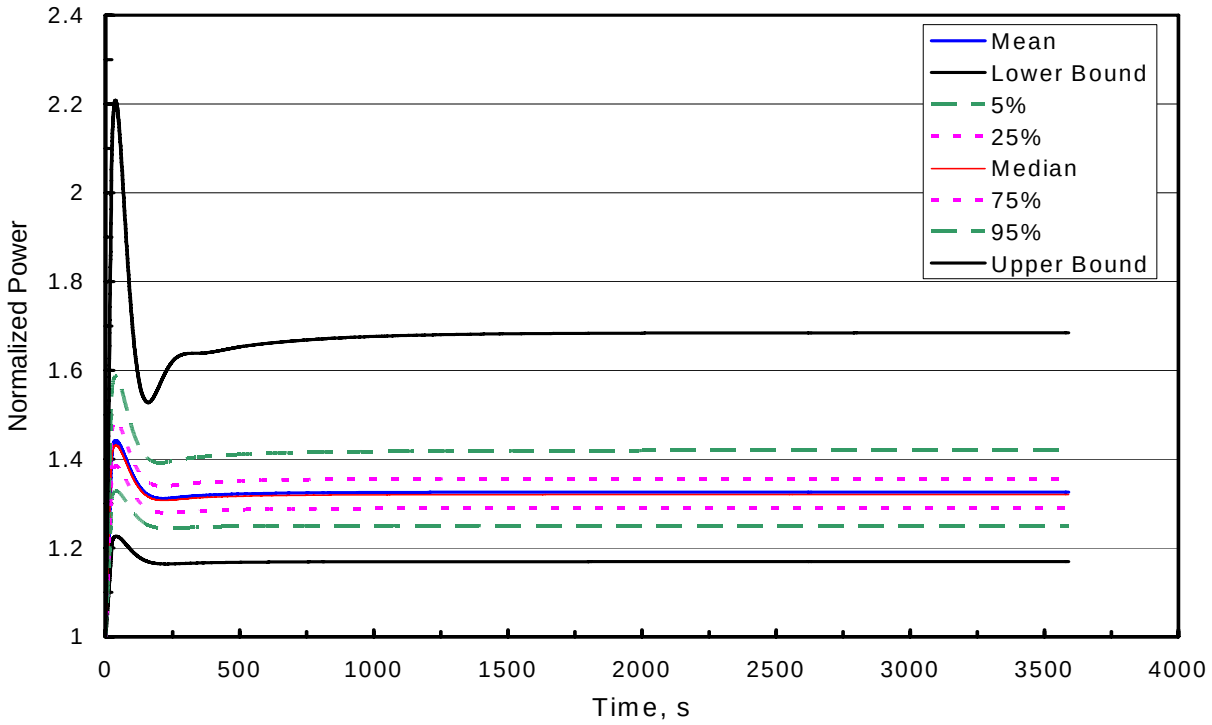

Fig. 21. Mean, percentiles and upper and lower bounds for the normalized power in a UTOP transient.

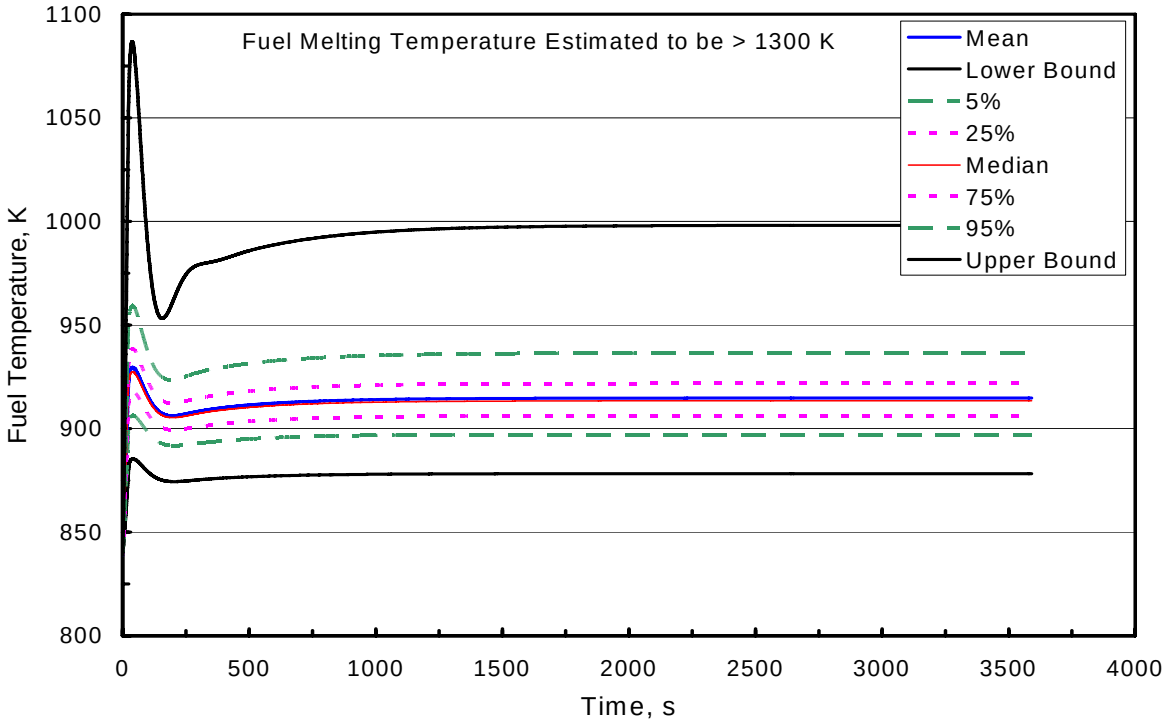

Fig. 22. Mean, percentiles and upper and lower bounds for the fuel temperature in a UTOP transient.

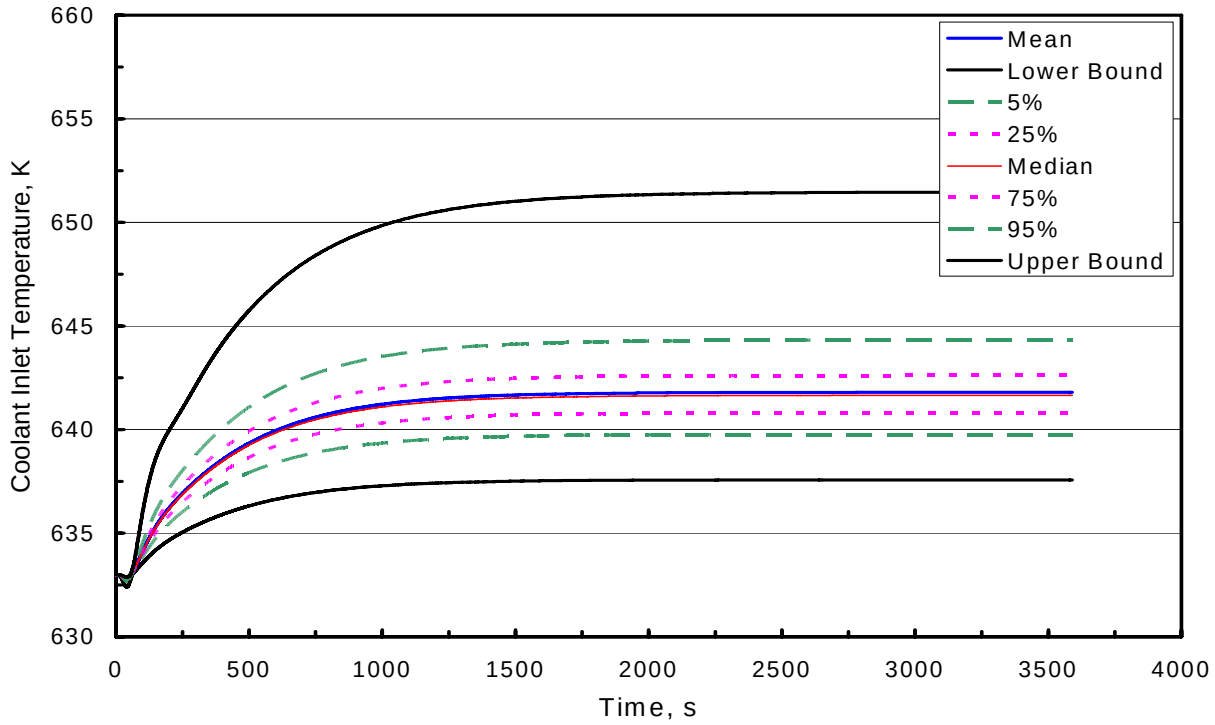

Fig. 23. Mean, percentiles and upper and lower bounds for the coolant inlet temperature in a UTOP transient.

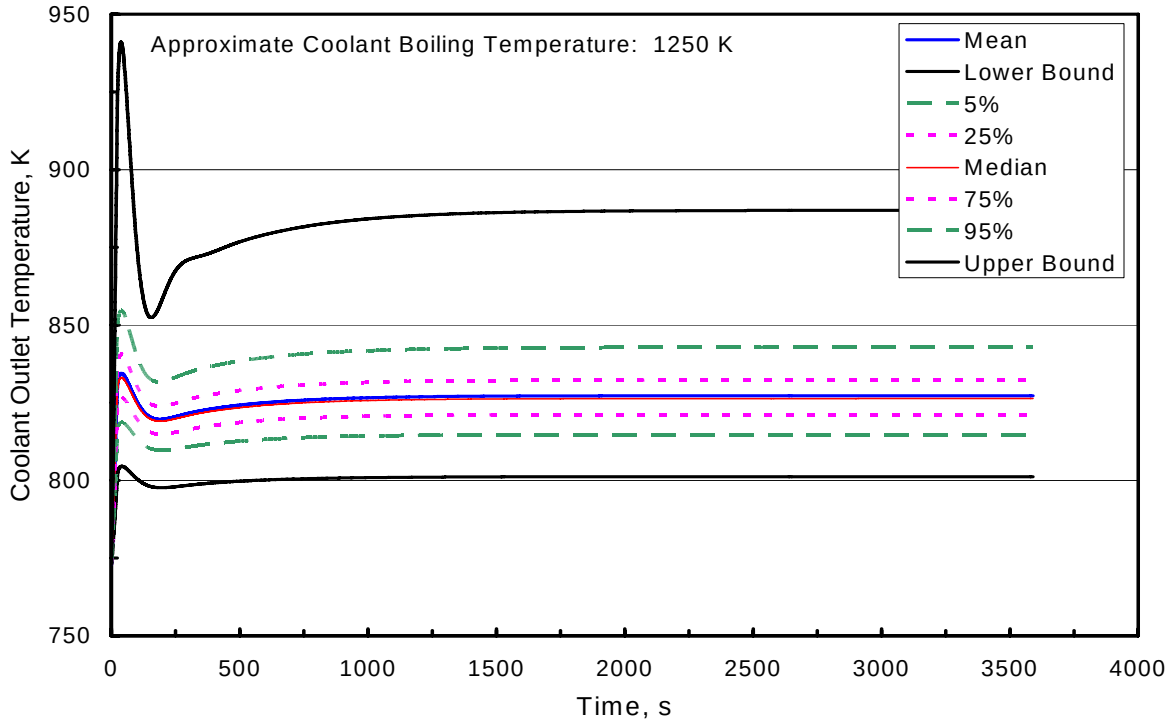

Fig. 24. Mean, percentiles and upper and lower bounds for the coolant outlet temperature in a UTOP transient.

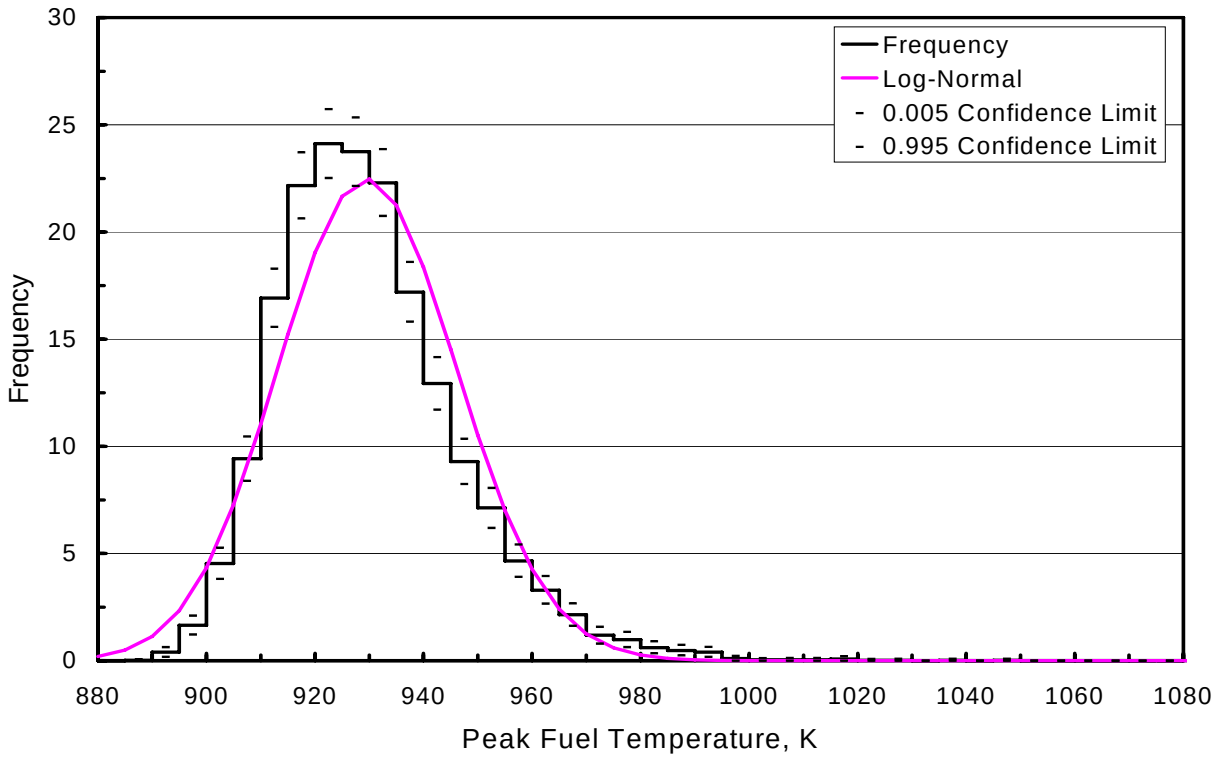

Fig. 25. Frequency distribution for the peak fuel temperature in a UTOP transient.

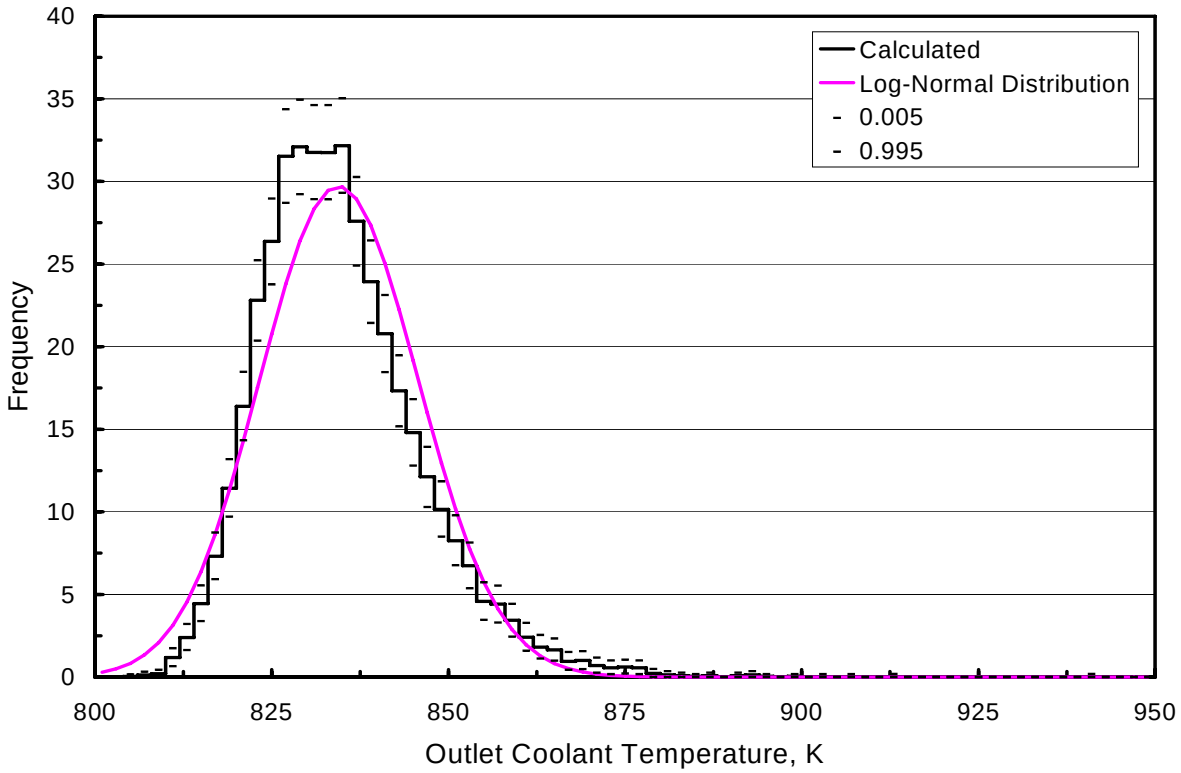

Fig. 26. Frequency distribution for the peak outlet coolant temperature in a UTOP transient.

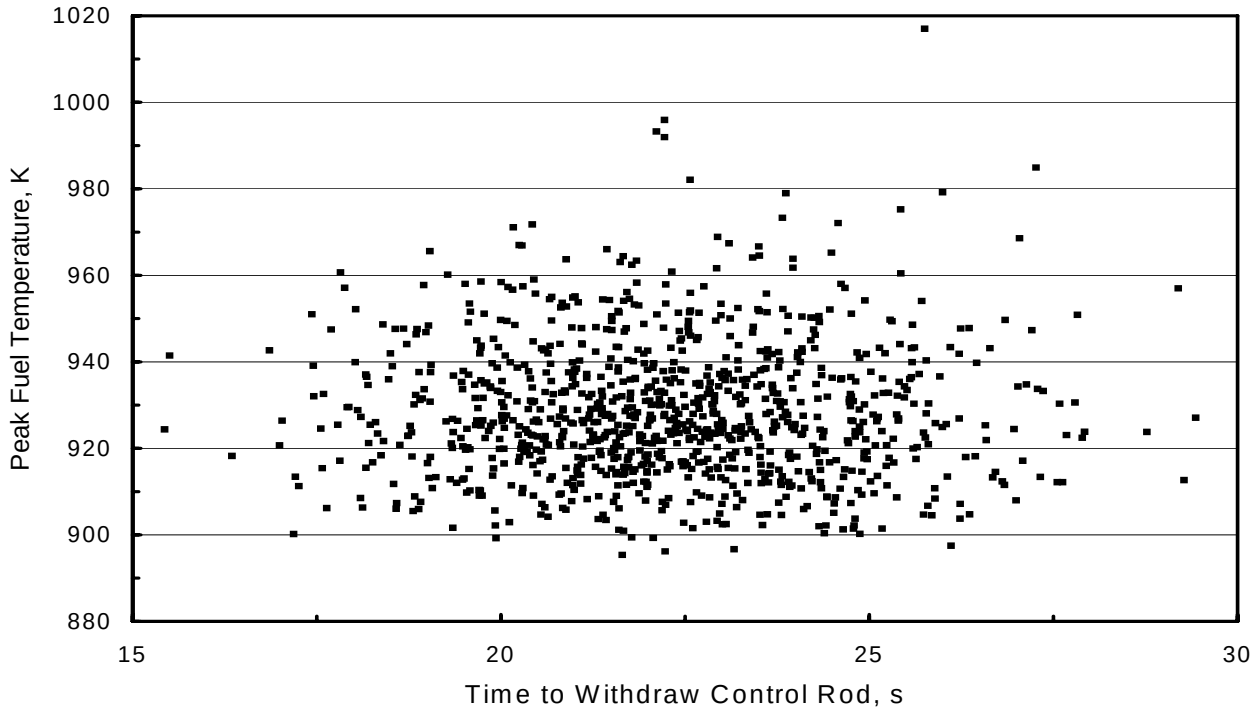

Fig. 27. Peak fuel temperature and the time required to withdraw a control rod for the first 1000 realizations in a UTOP transient.

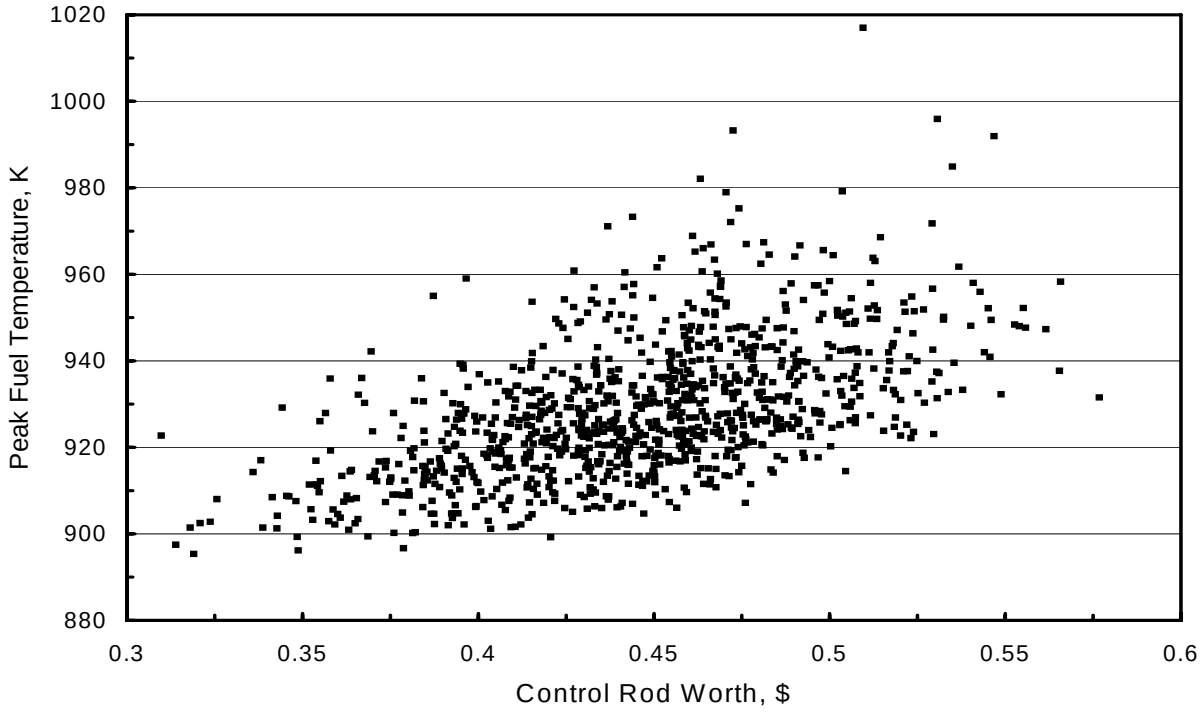

Fig. 28. Peak fuel temperature and control rod worth for the first 1000 realizations in a UTOP transient.

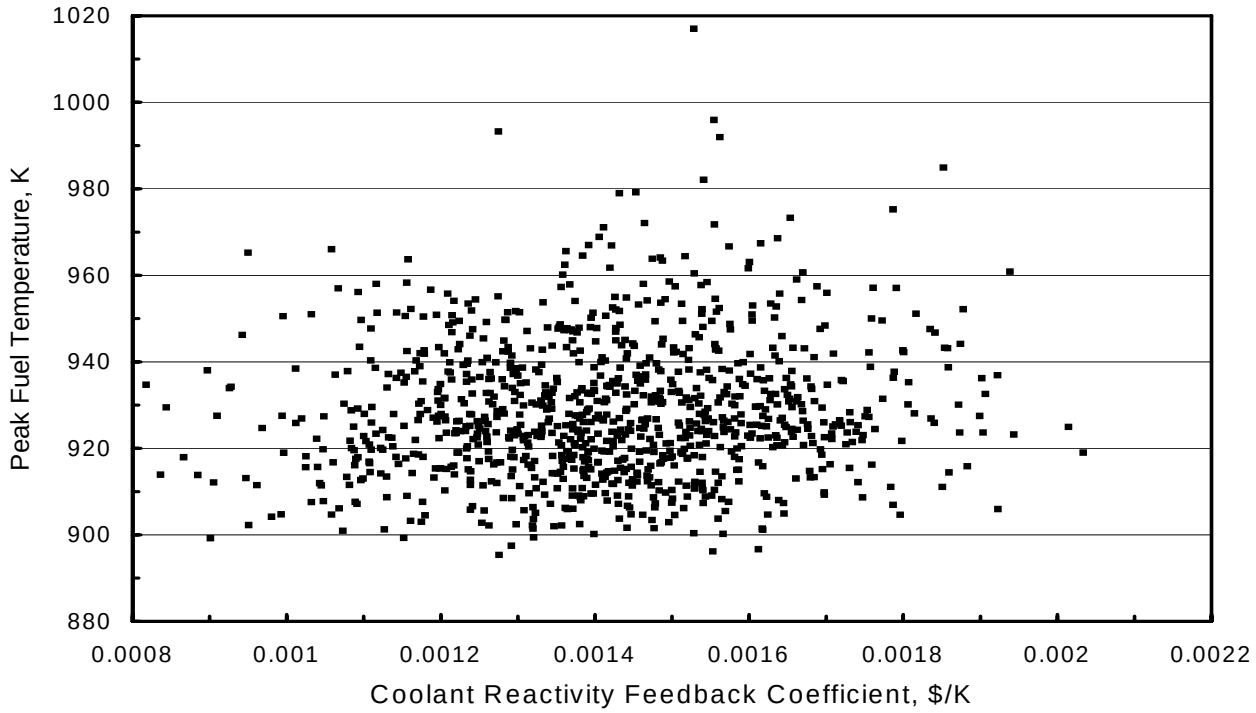

Fig. 29. Peak coolant outlet temerature and the coolant temperature reactivity feedback coefficient for the first 1000 realizations in a UTOP transient.

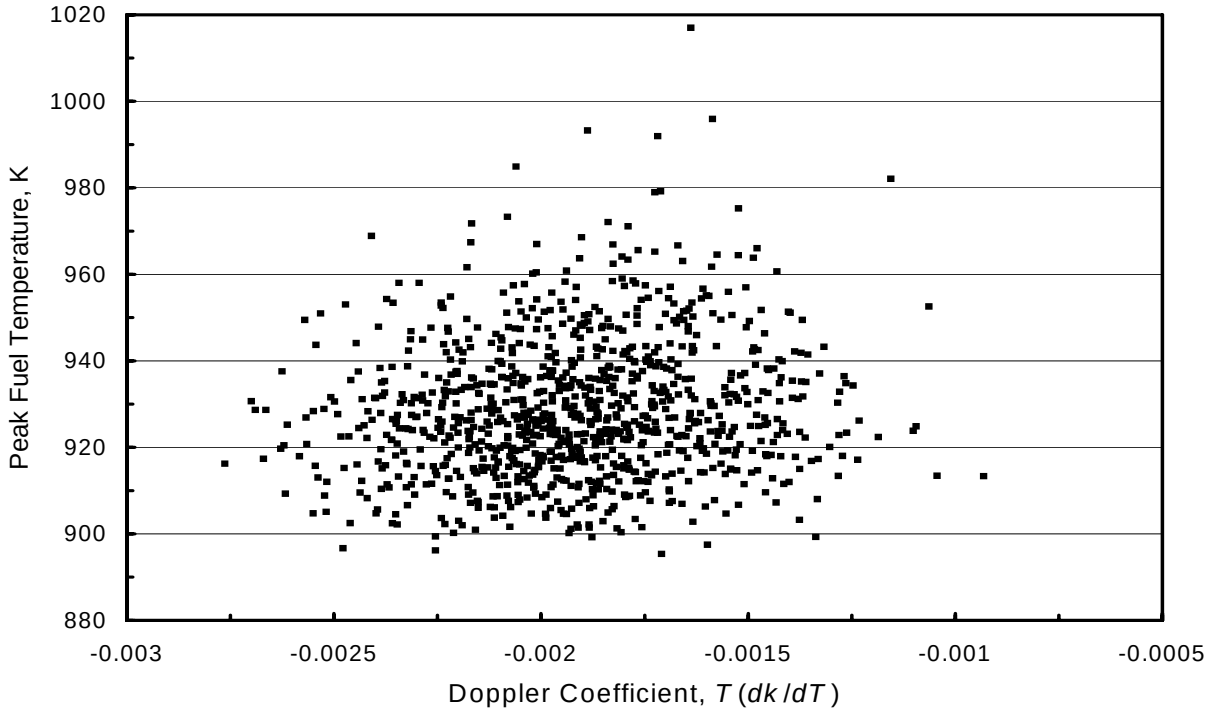

Fig. 30. Peak coolant outlet temperature and the Doppler reactivity feedback coefficient for the first 1000 realizations in a UTOP transient.

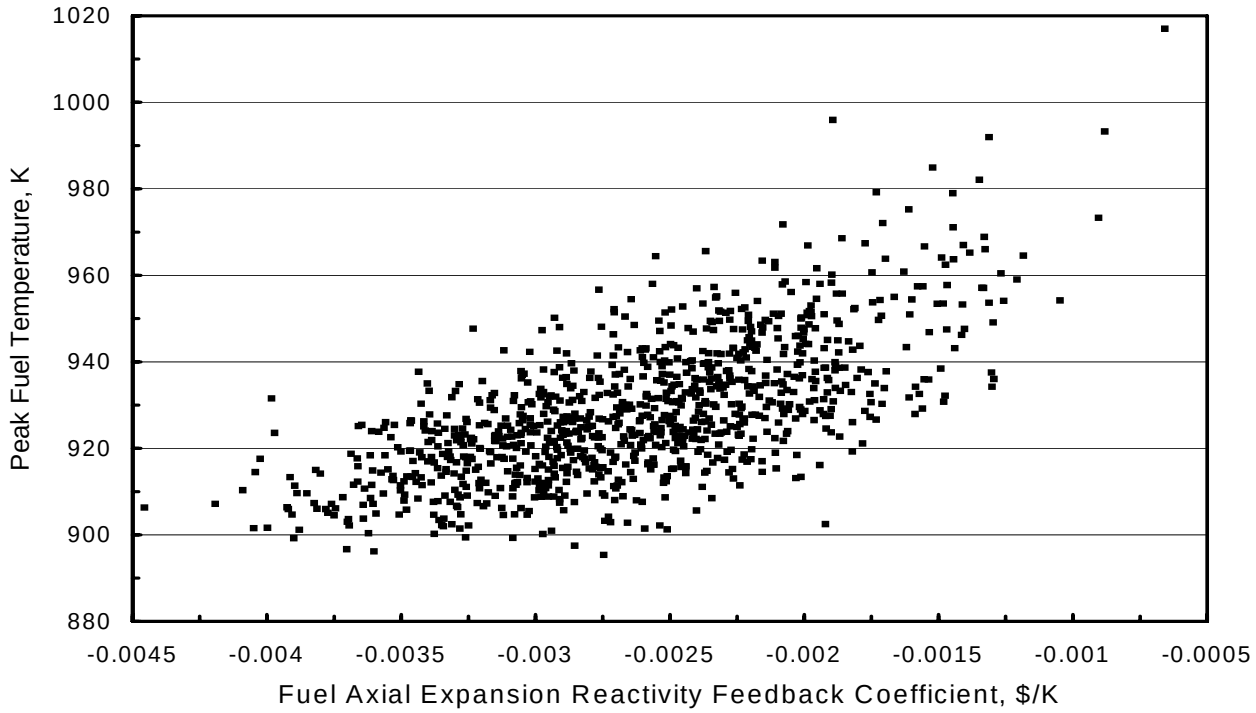

Fig. 31. Peak coolant outlet temperature and the fuel axial expansion reactivity feedback coefficient for the first 1000 realizations in a UTOP transient.

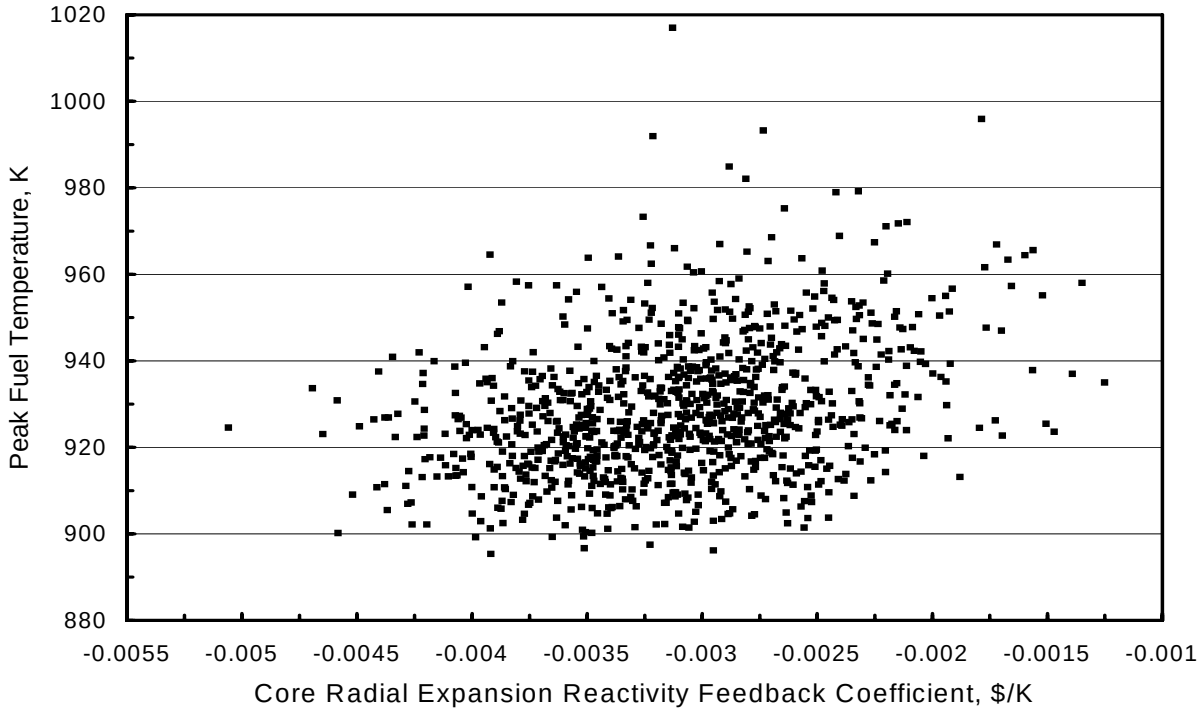

Fig. 32. Peak coolant outlet temperature and the core radial expansion reactivity feedback coefficient for the first 1000 realizations in a UTOP transient.

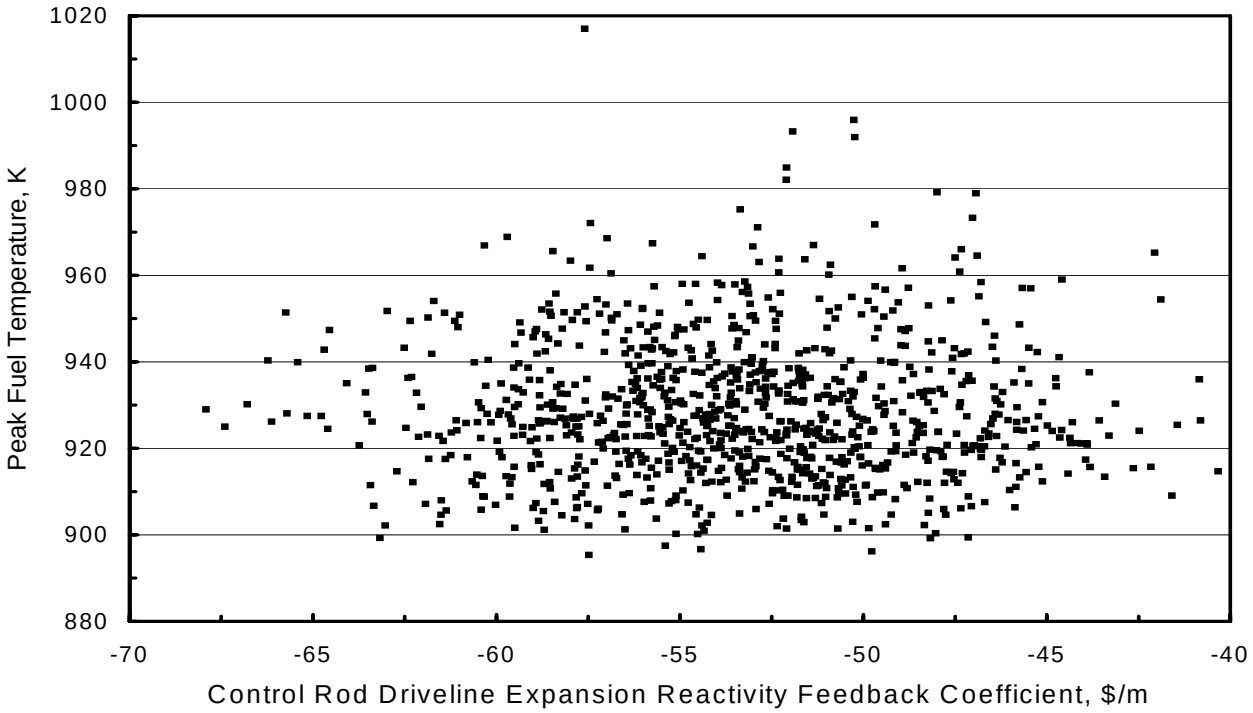

Fig. 33. Peak coolant outlet temperature and the control rod driveline expansion reactivity feedback coefficient for the first 1000 realizations in a UTOP transient.